Technical Report

TR-98-15

Studies of surface complexation of H^+, NpO_2^+, Co^{2+}, Th^{4+} onto TiO_2 and H^+, UO_2^{2+} onto alumina

Anna-Maria Jakobsson, Yngve Albinsson

Department of Nuclear Chemistry
Chalmers University of Technology, Sweden

and

Robert S Rundberg

Los Alamos National Laboratory, USA

November 1998

Svensk Kärnbränslehantering AB
Swedish Nuclear Fuel
and Waste Management Co
Box 5864
SE-102 40 Stockholm Sweden
Tel 08-459 84 00
+46 8 459 84 00
Fax 08-661 57 19
+46 8 661 57 19

Studies of surface complexation of H^+, NpO_2^+, Co^{2+}, Th^{4+} onto TiO_2 and H^+, UO_2^{2+} onto alumina

Anna-Maria Jakobsson, Yngve Albinsson

Department of Nuclear Chemistry
Chalmers University of Technology, Sweden

and

Robert S Rundberg

Los Alamos National Laboratory, USA

November 1998

Abstract

This report describes the determination of surface complexation reactions of some radionuclides on mineral oxides from sorption experiments and potentiometric titrations.

The surface acidity constants of the mineral oxide have been determined using potentiometric titrations. A description and discussion of the extrapolation method used is included as well as the calibration method which is of uttermost importance for calculating the constants. In this report it is shown that the data close to pH_{pzc} can not be used to calculate the apparent equilibrium constants since the assumption that either the positive or negative sites dominate gives rise to a pK^{app} that approach infinity. Furthermore it is shown that it is a fair estimation to assume a linear relationship between the inner surface charge and the potential since pure titanium dioxide gives a pK^{app} that has a linear dependence on the inner surface charge. Besides the surface acidity constants, the capacitance of the inner layer has been calculated from this linear dependence. The values of these agree well with other proposed in the literature.

The sorption of cobalt, thorium and neptunyl ions onto titanium dioxide and uranyl ions onto alumina from aqueous solution was studied as a function of pH and ionic strength in a CO_2 free environment at moderate radionuclide concentrations. Two different experimental methods were employed; an on-line method in which samples withdrawn at a specific pH are separated and measured, and a batch method. There is no significant difference between the average results from the two methods, however the on-line method provides less scatter. Also, using this method we were able to study the desorption easily and thus the reversibility of the reactions. There is no difference in sorption between the different ionic strengths for Np, Th, Co and U ions. This indicates the formation of inner sphere complexes with the surface. Neptunyl ion forms a neutral complex with the titanium dioxide and cobalt ion forms a complex with a positive charge at the inner surface. The sorption of thorium, neptunyl and cobalt ions has been shown in this work to be quantitatively controlled by the hydrolysis if no other strong complexing agents are present. The sorption of U was studied at varying concentrations ($9x10^{-11}$ - $5x10^{-8}$ M) and there was no observed difference in the sorption behavior indicating that there are no low density high energy sites affecting the surface complexation.

Key words: Surface Complexation, Th, Np, Co, U, Alumina, TiO_2, Sorption.

Sammanfattning

Rapporten beskriver studier av ytkomplexeringsreaktioner för vissa radionuklider på mineraloxider utifrån sorptionsexperiment och potentiometriska titreringar.

Mineraloxidytans syrakonstanter har bestämts med potentiometriska titreringar. Extrapolationsmetoden beskrivs och diskuteras. Kalibreringsmetoden för elektroderna som är viktig för beräkningen av konstanterna, är också beskriven. I denna rapport visas att data nära noll-laddningspunkten inte kan användas för bestämning av den apparenta (skenbara) jämviktskonstanten eftersom det normala antagandet att antingen de positiva eller negativa ytsätena dominerar ger upphov till ett pK^{app} som går mot oändligheten. Vidare visas det att det är rimligt att anta ett linjärt samband mellan laddning och potential eftersom pK^{app} för ren titandioxid är linjärt beroende av laddningen. Förutom ytans syrakonstanter har det inre lagrets kapacitans beräknats. Värdena är väl överensstämmande med litteraturvärden.

Sorptionen av kobolt, torium och neptunium på titandioxid och uran på aluminiumoxid från vattenlösningar har studerats som funktion av pH och jonstyrka i en CO_2-fri miljö vid moderata radionuklidkoncentrationer. Två olika experimentella förfaranden har använts: en on-line metod där prov tas från samma lösning vid olika specifika pH:n, separeras och mäts, och en batch metod där pH:t mäts i de individuellt beredda proverna efter fasseparation. Förutom att on-line metoden ger mindre spridning i data uppvisade resultaten ingen skillnad mellan de olika metoderna. Fördelen med on-line metoden är att desorptionen, och därmed reversibiliteten, lätt kan mätas. Sorptionen av Np, Th, Co och U påverkades ej av olika jonstyrkor. Detta tyder på att de alla bildar innersfärskomplex med ytan. Neptunyl bildar ett oladdat komplex och kobalt ett positivt laddat. Sorptionen av Th, Np och Co joner är kvantitativt kontrollerad av hydrolysen om inga andra starka komplexbildare är närvarande. Sorptionen av U studerades över varierande koncentrationer ($9x10^{-11}$ - $5x10^{-8}$ M) och ingen skillnad i sorptionen observerades vilket tyder på att det inte finns några lågdensitets högenergi säten som påverkar sorptionen.

TABLE OF CONTENTS

1 Introduction

In the performance assessment of a repository for spent nuclear fuel, one of the main problems is to predict to what extent radionuclides released from the fuel will migrate through the surrounding rock. One of the controlling factors is the sorption of the different elements onto the minerals present along the water bearing fractures. In order to predict the sorption under varying conditions it is important to understand the sorption mechanisms and magnitude. Information can be provided by surface complexation studies whereby the sorption mechanisms on simple mineral oxides are often seen as formation of complexes with the surface OH groups, similar to hydrolysis reactions /Dzombak and Morel, 1990/.

The sorption of an ion on a given surface will, among others, be affected by the pH, electrolyte concentration, and the concentration of complexing ligands. The pH affects the hydrolysis both of the ions and the surface, which influences the sorption. The electrolyte concentration affects the solid-liquid interface layer and the extent of the effect on the sorption depends on the type of surface complex formed. To reduce the complexity of the system the concentration of carbonate, which is a complexing ligand, has been kept as low as possible in this work.

The pH affects the charge of the surface due to the amphoteric nature of the mineral oxides. The equilibrium constants for these surface acidity reactions are determined by potentiometric titrations. This work describes the determination of acidity constants using potentiometric titrations exemplified by TiO_2 and sorption studies of UO_2^{2+} onto alumina and Np, Co and Th onto TiO_2 as a function of pH at different ionic strengths.

Titanium dioxide was chosen because i) it has a very low solubility and thus the surface complexation can be studied at a wide pH interval without the interference of dissolution and ii) it has a pH_{pzc} between the high value of alumina and iron oxides and the low of silica oxides. These properties admit sorption studies over a wide pH interval and an inter-comparison between different elements can be made. Alumina was chosen because i) it is present to a large degree in fracture filling materials and will thus have an influence on the migration from a repository of spent nuclear fuel and ii) to represent mineral oxides of a high pH_{pzc}.

The ions that have been studied are NpO_2^+, Co^{2+}, Th^{4+} and UO_2^{2+}. All except Th are major parts of the element inventory in the spent fuel and represent three different effective charges. ^{237}Np will, due to its long half-life, be one of the dominating source of radioactivity in the waste after about 10^5 years. Cobalt and thorium represent divalent and tetravalent cations, respectively.

2 General theory

The amphoteric nature of mineral oxides can be described with the following reactions:

$$\equiv SOH_2^+ \longleftrightarrow \equiv SOH + H^+ \qquad K_{a1}^{int} = \frac{\{\equiv SOH\}\{H^+\}}{\{\equiv SOH_2^+\}} \qquad [2\text{-}1]$$

$$\equiv SOH \longleftrightarrow \equiv SO^- + H^+ \qquad K_{a2}^{int} = \frac{\{\equiv SO^-\}\{H^+\}}{\{\equiv SOH\}} \qquad [2\text{-}2]$$

where $\equiv SOH$ denotes surface species, $\{i\}$ the activity of the species i at the surface, and K_{a1}^{int} and K_{a2}^{int} are the intrinsic equilibrium constants. (That is the actual equilibrium constants with respect to the activities at the reaction sites.) The surface will acquire an electric charge, σ, due to these reactions and there will be a potential difference between the surface and the bulk. The pH at which the number of positive sites is equal to the number of negative sites (and thus the net inner surface charge is zero) is the point of zero charge, pH_{pzc}. If the only potential determining ions are the H^+ and OH^- the pH_{pzc} will relate to the intrinsic equilibrium constants by:

$$pH_{pzc} = (pK_{a1} + pK_{a2}) / 2 \qquad [2\text{-}3]$$

(where pK = -log K). There are a number of different models of varying complexity describing the potential and charge of the surface-liquid interface such as the Constant Capacitance Model (CCM), Diffuse Layer Model (DLM), Stern model and Triple Layer Model (TLM).

The interface can be described as a constant capacitance layer, a diffuse layer or a combination of these. In the constant capacitance model (Helmholtz) the surface interface is described by one layer with a constant capacitance. The potential decreases linearly with the distance from the surface. The diffuse layer model (Gouy-Chapman) describes the interface as consisting of a diffuse layer and the Stern model consists of one constant capacitance layer and one diffuse. In the triple layer model the surface is described with three different layers; 2 of constant capacitance (inner and outer Helmholtz) and one diffuse layer, confined by three planes, 0-, β– (inner Helmholtz plane), and d-plane (outer Helmholtz plane), and by the bulk (see Figure 2-1). Only the TLM distinguishes between inner and outer sphere complexes.

At the 0-plane the potential determining ions (p.d.i.) ($\equiv SOH_2^+$ and $\equiv SO^-$) and species forming inner sphere complexes are located /Hayes and Leckie, 1987/, /Grahame, 1947/. Formation of an inner sphere complex with a positive ion Q of charge z can be described by:

$$\equiv SOH + Q^{z+} + bH_2O \longleftrightarrow (\equiv SO)(H)_c\, Q(OH)_b^{z-b} + (1 - c + b)H^+ \qquad [2\text{-}4]$$

The equilibrium constant for the reaction is:

$$K_Q^{int} = \frac{\left\{(\equiv SO)(H)_c Q(OH)_b^{z-b}\right\}\{H^+_{0-plane}\}^{1-c+b}}{\{\equiv SOH\}\{Q^{z+}_{0-plane}\}} \qquad [2\text{-}5]$$

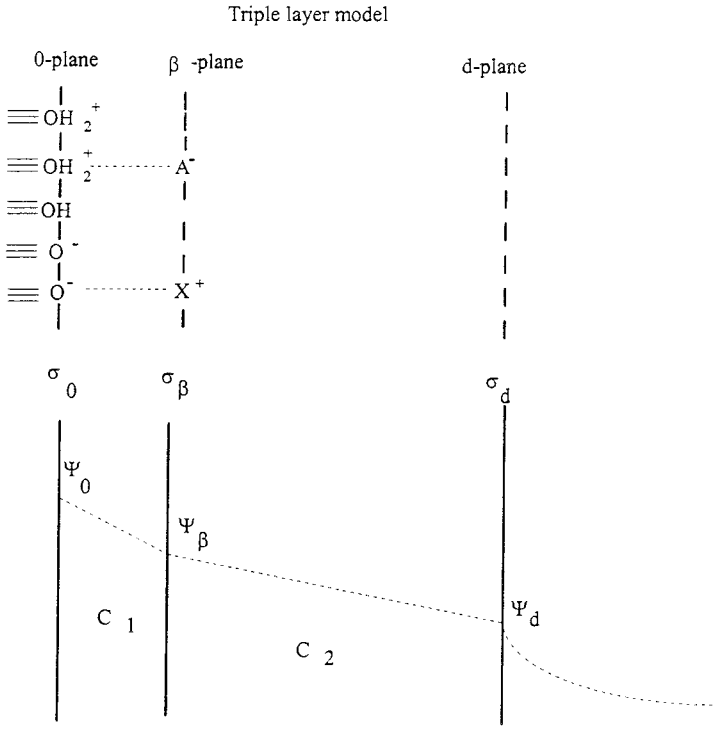

Figure 2.1. *The triple layer model, C_1 and C_2 are the capacitances of the inner and outer Helmholtz layers. Ψ_i denotes the potential and σ_i the charge at the plane i. The charges are related to each other by the electroneutrality: $\sigma_0 + \sigma_\beta + \sigma_d = 0$.*

Due to the charge of the surface, ions in the solution will be attracted and form electrostatic type of complexes with the surface. The ions that are associated with specific surface sites (forming ion-pair complexes and outer sphere complexes) are located at the β-plane. These contribute to the charge σ_β. The reaction with the supporting electrolyte (X^+: cation, A^-: anion) can be described as:

$$\equiv SOH_2^+ + A^- \longleftrightarrow \equiv SOH_2^+A^- \qquad K^{int}_{A-} = \frac{\left\{\equiv SOH_2^+ A^-\right\}}{\left\{\equiv SOH_2^+\right\}\left\{A^-_{\beta-plane}\right\}} \qquad [2\text{-}6]$$

$$\equiv SO^- + X^+ \longleftrightarrow \equiv SO^- X^+ \qquad K^{int}_{X+} = \frac{\left\{\equiv SO^- X^+\right\}}{\left\{\equiv SO^-\right\}\left\{X^+_{\beta-plane}\right\}} \qquad [2\text{-}7]$$

where K^{int}_{A-} and K^{int}_{X+} are the intrinsic constants for the formation of complexes with the supporting electrolyte.

Outside the d-plane the ions move freely but are affected by the charge of the surface. The resulting distribution of the ions in the layers due to the potential differences can be described by a Boltzmann distribution. The activity of an ion, $\{X^{z+}\}$, at a plane i ($i = 0$, β, d) will depend on the potential Ψ_i:

$$\left\{X^{z+}_{i\text{-}plane}\right\} = \left\{X^{z+}_{bulk}\right\} e^{-\frac{zF\Psi_i}{RT}} \qquad [2\text{-}8]$$

From this equation the relationship between the intrinsic equilibrium constant of a surface reaction and the apparent one can be found. Thus, the first surface acidity reaction the apparent and the intrinsic constants are related as:

$$K^{\text{int}}_{a1} = K^{app}_{a1} e^{\frac{-F\Psi_0}{RT}} \qquad [2\text{-}9]$$

or taking the negative log of both sides:

$$pK^{\text{int}}_{a1} = pK^{app}_{a1} + \frac{F\Psi_0}{RT\ln 10} \qquad [2\text{-}10]$$

The intrinsic constant for the surface acidity reactions can thus be determined by extrapolation to zero potential. Commonly this is done as proposed in /Davis, James and Leckie, 1978/ by extrapolation to zero inner surface charge as this is a quantity that can be calculated from titrations. In the triple layer model the two inner layers are seen as two plate capacitors of constant capacitance, C_1 and C_2. These give the relationship between the charges of the different planes and the potential as:

$$\Psi_0 - \Psi_\beta = \sigma_0 / C_1 \qquad [2\text{-}11]$$

$$\Psi_\beta - \Psi_d = \sigma_d / C_2 \qquad [2\text{-}12]$$

Substitution of [2-11] in [2-10] gives:

$$pK^{\text{int}}_{a1} = pK^{app}_{a1} + \frac{F(\Psi_\beta + \sigma_0 / C_1)}{\ln(10)RT} \qquad [2\text{-}13]$$

The intrinsic constant pK^{int} can be found by extrapolating eq. [2-13] to zero inner surface charge (assuming that the potential at the β-plane, Ψ_β , is zero at $\sigma_0 = 0$). From the slope of the extrapolation the capacitance, C_1, can be calculated. Care has to be taken in the choice of data points that are used in the extrapolation. Close to pH_{pzc} the apparent equilibrium constants can not be calculated as is pointed out in Section 4.1.6.

Since the determination of the surface constants is highly dependent on an accurate measurement of the actual H^+ concentration in the solution, it is important to make a good calibration of the electrode response to the H^+ concentration. This procedure has

been assigned a section of its own (Section 3).

In a titration the deficit or surplus of H^+ due to the reactions [2-1] and [2-2] is measured as a function of pH. From this the apparent equilibrium constants and the inner surface charge can be calculated, and from these the intrinsic constants can be found by extrapolation to zero inner surface charge. This is described in Section 4.

In sorption studies the distribution of the sorbing species between the aqueous and solid phase is measured as a function of pH and ionic strength. The advantages of using the distribution coefficient, K_d in studies of sorption are that it can be experimentally determined directly without any speciation calculations and that it will give an indication about the type of complex that will be formed. If the distribution coefficient is corrected for the surface area an inter-comparison between different minerals can be made and the influence of their chemistry on the sorption can be studied. Such an inter-comparison between various experiments using percentage of sorption requires the same experimental conditions (concentration of nuclide, and solid to solution ratio).

The distribution coefficient, K_d is related to the equilibrium constant of the surface complexation reaction. A relationship between the K_d, the apparent equilibrium constant, K^{app}, and the pH can be derived as follows. The K_d can be expressed as:

$$K_d = \frac{[surface\ complex]}{[x]_{totaq}} * \frac{S_{mol}}{[SOH_{tot}]} \qquad [2\text{-}14]$$

where x is the sorbing species, $[i]$ is the concentration of species i, $[SOH_{tot}]$ is the total concentration of surface sites, and S_{mol} is site density in mol sites per mass. The K^{app} for a reaction involving the release of y protons is:

$$K^{app} = \frac{[surface\ complex][H^+]^y}{[x^{z+}]_{aq}[SOH]} \qquad [2\text{-}15]$$

To relate the K^{app} and K_d mass balances for the different species are required.

1. Mass balance for surface sites (assuming that all are amphoteric and can be involved in the different reactions and that only one site is involved in the surface complexation reaction):

$$[SOH]_{tot} = [SOH_2^+] + [SOH] + [SO^-] + [surface\ complex] \qquad [2\text{-}16]$$

Assuming that the concentration of the sorbing species is negligible in comparison to the surface hydroxyl site concentration the mass balance [2-16] can be rewritten as:

$$[SOH]_{tot} = [SOH]\left(\frac{K^s_{a2}}{[H^+]} + 1 + \frac{[H^+]}{K^s_{a1}}\right) \qquad [2\text{-}17]$$

2. Mass balance over the total concentration of the sorbing species in the aqueous phase:

$$[x]_{totaq} = [x^{z+}]_{aq} + [x(OH)^{(z-1)+}]_{aq} + [x(OH)_2{}^{(z-2)+}]_{aq} + \ldots =$$
$$= [x^{z+}]_{aq}\left(1 + \frac{K_{a1}}{[H^+]} + \frac{K_{a2}}{[H^+]^2} + \frac{K_{a3}}{[H^+]^3} + \ldots\right) \qquad [2\text{-}18]$$

where K_{a1}, K_{a2} etc. are the hydrolysis constants for the sorbing species (assuming that no poly nuclear complexes are formed.)

Combining [2-14], [2-15] and the mass balances gives:

$$\log K_d = \log K^{app} + y\,\mathrm{pH} + \log S_{mol} - \log\left(1 + \frac{K_{a1}}{[H^+]} + \frac{K_{a2}}{[H^+]^2} + \frac{K_{a3}}{[H^+]^3} + \ldots\right) - \log\left(1 + \frac{K^s_{a2}}{[H^+]} + \frac{[H^+]}{K^s_{a1}}\right) \qquad [2\text{-}19]$$

which can be rewritten as:

$$\log K_d = \log K^{app} + y\,\mathrm{pH} + \log S_{mol} - \log\left(1 + 10^{(\mathrm{pH-pKa1})} + 10^{(2\mathrm{pH-pKa2})} + 10^{(3\mathrm{pH-pKa3})} + \ldots\right) -$$
$$- \log\left(1 + 10^{(\mathrm{pH-pKsa2})} + 10^{(\mathrm{pKsa1-pH})}\right) \qquad [2\text{-}20]$$

The fraction of the activity coefficients of the surface species is set to unity /Dzombak and Morel, 1990/. The activity coefficients for the H^+, OH^- and supporting electrolyte have been calculated using Pitzers equations /Pitzer, 1991/ for the titrations.

3 Calibration of the electrode

Prior to all titrations of the surface the electrode response is calibrated under the same conditions using a method based on Gran calibrations /Gran, 1950/, /Gran 1952/. The steps in a traditional Gran calibration are:

i) The equivalence volume is found by extrapolation of the Gran functions to zero. The equivalence volume is the volume of base needed to neutralize the acid. The Gran functions are actually just linear functions of the moles of H^+ or OH^-. From this the concentration of the base is calculated.

ii) Once the concentrations are known of all the species the coefficients for the relationship between the potential and H^+ / OH^- concentrations are found by for example linear regression.

In the method used in this work the equivalence volume is found together with the coefficients by a least squares fit. Thus only one regression and fit is required.

The first section will give a brief derivation of the equations relating the H^+ and OH^- concentrations to the electrode response. The second part is a description of Gran calibrations and the third part describes the method used in this work. The fourth part is an illustration of the use of Gran functions to see how good the titration was and how to estimate the amount of carbonate in the base.

Throughout the rest of the report pH will refer to the negative logarithm of the H^+ concentration.

3.1 The electrode response

The following relationships are for constant temperature and pressure. The potential difference measured is the result of the differences at all the junctions:

$$E = E_{R.E.} + E_j + E_{G.E} \qquad [3\text{-}1]$$

where $E_{R.E.}$ is the potential difference between the reference electrode and the reference solution, E_j the potential over the junction between the titrated solution and the outer reference solution and $E_{G.E.}$ the potential between the glass electrode and the titrated solution.

system:ref. electrode (R.E.) | ref. soln.: titrated soln. | glass electrode (G.E.)
potentials: $E_{R.E.}$ E_j $E_{G.E.}$

The glass electrode potential, $E_{G.E.}$, is a function of the H^+ activity in the solution (Nernst equation):

$$E_{G.E.} = E^{o}_{G.E} - \eta \frac{RT}{F} \ln\{H+\} = E^{o}_{G.E} - \eta s \log \{H+\} \qquad [3\text{-}2]$$

where $s = RT/F \ln 10$ and η is the efficiency of the electrode. The liquid junction potential, E_j, arises from the difference in mobilities of the different ions. Using the Henderson approximation /Bates, 1973/ for high concentrations, linearizing the H^+ dependence, the junction potential can be expressed as:

$$E_j = E^{o}_{j} + \Phi_a [H^+] \qquad \text{at low pH and} \qquad [3\text{-}3]$$

$$E_j = E^{o}_{j} + \Phi_b [OH^-] \qquad \text{at high pH} \qquad [3\text{-}4]$$

where Φ_a and Φ_b are the coefficients for the dependence of the liquid junction potential of the H^+ and OH^- concentrations. The reference potential, $E_{R.E.}$, is constant throughout the titration.

All the constants can be combined into one:

$$E^{o} = E_{R.E.} + E^{o}_{j} + E^{o}_{G.E} \qquad [3\text{-}5]$$

Substitution of [3-2], [3-3] and [3-5] in [3-1] gives at the acid side:

$$E = E^{o} - \eta s \log\{H^+\} + \Phi_a [H^+] = E^{o} - \eta s \log[H^+] - \eta s \log \gamma_{H+} + \Phi_a [H^+] \qquad [3\text{-}6]$$

where γ_{H^+} is the activity factor. If the titration is performed at a constant ionic strength the activity factor for the H^+ will be nearly constant as well and can be included in a constant term for the acid side, E_0:

$$E_0 = E^{o} - \eta s \log \gamma_{H+} \qquad [3\text{-}7]$$

which substituted in [3-6] gives the final relationship between the electrode response and the H^+ concentration:

$$E = E_0 - \eta s \log [H^+] + \Phi_a [H^+] \qquad [3\text{-}8]$$

At the base side a similar relationship to the OH^- concentration can be found by substituting the H^+ concentration with the water ionization product, $K_w = \{OH^-\} * \{H^+\}$, [3-2], [3-4] and [3-5] in [3-1]:

$$E = E^{o} + \eta s \log[OH^-] + \eta s \log \gamma_{OH-} - \eta s \log K_w + \Phi_b [OH^-] \qquad [3\text{-}9]$$

At constant temperature and ionic strength γ_{OH-} is constant. All the constant terms can be combined into one, E'_0:

$$E'_0 = E^o - \eta s \log K_w + \eta s \log \gamma_{OH-} \quad [3\text{-}10]$$

Thus the final expression for the relationship between the electrode response and the OH^- concentrations is:

$$E = E_0^{'} + \eta s \log\left[OH^-\right] + \Phi_b\left[OH^-\right] \quad [3\text{-}11]$$

The relationship between the two constant terms E_0 and E'_0 can be used to find the water ionization product at a certain ionic strength, $Q_w=[OH^-]*[H^+]$, from:

$$\log Q_w = \log K_w - \log \gamma_{OH-} - \log \gamma_{H+} = \frac{E_0 - E'_0}{\eta s} \quad [3\text{-}12]$$

3.2 Gran calibration

The following description is based on the use of Gran functions to determine the concentration of a strong base, c_b, titrating a strong acid, c_a. In Gran titrations the concentration is determined by finding the equivalence volume of base, v_e, needed to neutralize the acid:

$$v_e = \frac{v_a c_a}{c_b} \quad [3\text{-}13]$$

where v_a is the volume of added acid. The number of moles of H^+ is at the acid side:

$$\text{mol}_{H+} = v_a c_a - v_b c_b = v_a c_a (1 - \frac{v_b}{v_e}) \quad [3\text{-}14]$$

and the number of moles of OH^- is at the base side:

$$\text{mol}_{OH-} = v_b c_b - v_a c_a = v_a c_a (\frac{v_b}{v_e} - 1) \quad [3\text{-}15]$$

The Gran functions, F_1 (acid side) and F_2 (base side) are:

$$F_1 = v_{tot} 10^{-Es^{-1}} \quad [3\text{-}16]$$

$$F_2 = v_{tot} 10^{Es^{-1}} \quad [3\text{-}17]$$

These can be rewritten as functions of the added volume of base, v_b, by substituting for the acid side eq. [3-8] (assuming the efficiency of the electrode, η, to be 1) in [3-4]:

$$F_1 = v_{tot}(10^{-\text{pH}})(10^{(-E_0 - \Phi_a\left[H^+\right])s^{-1}}) \quad [3\text{-}18]$$

$$= \mathrm{mol}_{H+} 10^{-(E_0 - \Phi_a[H^+])s^{-1}} \quad [3\text{-}19]$$

$$= v_a c_a (1 - \frac{v_b}{v_e}) 10^{-(E_0 - \Phi_a[H^+])s^{-1}} \quad [3\text{-}20]$$

and for the base side eq. [3-10] in [3-5]:

$$F_2 = v_{tot} 10^{\mathrm{pOH}} 10^{(E'_0 + \Phi_b[OH^-])s^{-1}} \quad [3\text{-}21]$$

$$= \mathrm{mol}_{OH^-} 10^{(E'_0 + \Phi_b[OH^-])s^{-1}} \quad [3\text{-}22]$$

$$= v_a c_a (\frac{v_b}{v'_e} - 1) 10^{(E'_0 + \Phi_b[OH^-])s^{-1}} \quad [3\text{-}23]$$

F_1 and F_2 will be linear functions of the added amount of base if the liquid junction potential terms (Φ_a [H^+] and Φ_b [OH^-]) and Q_w are constant. Extrapolation of F_1 and F_2 to zero will give two equivalence volumes, v_e (from F_1) and v'_e (from F_2). These should be the same, but can deviate due to presence of carbonate in the base (see Section 3.4).

From the equivalence volume the concentration of H^+ and OH^- in each step of the titration can be calculated.

3.3 Calibrating the electrode with a least squares fit

The efficiency, the E_0 and the liquid junction potentials can be found by linear regression between the actual measured potential and the calculated one. This is done by minimizing the sum of the squares of the difference between the two, U:

$$U = \sum_n \left(E_{calc,n} - E_{meas,n} \right)^2 \quad [3\text{-}24]$$

The E_0 and E'_0 used for the calculated E are the averages of the E_0 and E'_0. On the acid side the calculated potential is

$$E_{calc,n} = \overline{E_0} - \eta s \log[H_n^+] + \Phi_a[H_n^+] \quad [3\text{-}25]$$

and on the base side it is:

$$E_{calc,n} = \overline{E'_0} + \eta s \log[OH_n^-] + \Phi_b[OH_n^-] \quad [3\text{-}26]$$

Substitution in eq. [3-24] together with [3-8] and [3-11] gives:

$$U = \sum_n \left(E_{calc,n} - E_{meas,n}\right)^2 = \sum_n \left(\overline{E_0} - E_{0,n}\right)^2 + \sum_n \left(\overline{E'_0} - E'_{0,n}\right)^2 \qquad [3\text{-}27]$$

where

$$E_0 = E + \eta s \log(v_a c_a (1 - \frac{v_b}{v_e}) v_{tot}^{-1}) + \Phi_a (v_a c_a (1 - \frac{v_b}{v_e}) v_{tot}^{-1}) \qquad [3\text{-}28]$$

and

$$E'_0 = E - \eta s \log(-v_a c_a (1 - \frac{v_b}{v'_e}) v_{tot}^{-1}) + \Phi_b (-v_a c_a (1 - \frac{v_b}{v'_e}) v_{tot}^{-1}) \qquad [3\text{-}29]$$

U is minimized by varying v_e, v'_e, η, Φ_b and Φ_a. E_0 and E'_0 are found from the average values and Q_w from equation [3-12]. The method is a further development of what was proposed by /Rossotti and Rossotti, 1965/, finding the equivalence volumes by trial and error varying v_e until E_0 is constant.

3.4 Estimation of the amount of carbonate present in the base

If carbonate is present the measured points will tend to deviate from the straight line at the equivalence volume, as can be seen in Figure 3.1, and the equivalence volumes v_e and v'_e will differ.

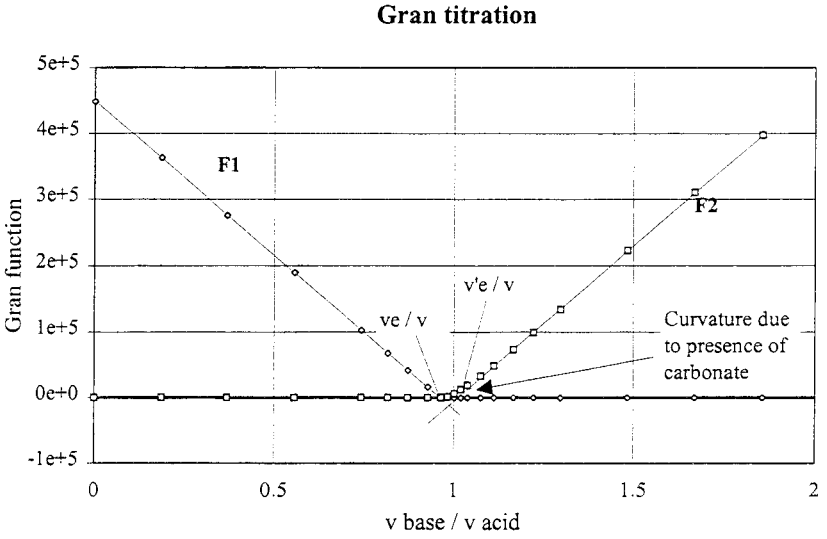

Figure 3.1 *The Gran functions F_1 and F_2 as a function of added base / added volume. By extrapolating the Gran functions to zero the equivalence volumes at the acid and base side are determined. If there is carbonate present in the base the F_2 function will curve. The amount can be estimated from the difference in the equivalence volumes.*

An estimation of the amount of carbonate present can be made from the difference in

the equivalence volumes since [ROS 65]:

$$v_e = \frac{v_a c_a}{c_b} \qquad \text{(acid side)} \qquad [3\text{-}30]$$

$$v_e' = \frac{v_a c_a}{c_b + 2\left[CO_3^{2-}\right]} = \frac{v_a c_a}{c_b'} \qquad \text{(base side)} \qquad [3\text{-}31]$$

leads to an estimation of the carbonate concentration from:

$$\left[CO_3^{2-}\right] = \frac{c_b' - c_b}{2} \qquad [3\text{-}32]$$

where c_b is the base concentration determined from the acid side and c_b' from the base side.

4 Determination of K^{int}_{a1} and K^{int}_{a2}

Two methods have been used to determine the protolysis constants from the titrations. One extrapolation method described in Section 4.1 and the program FITEQL /Westall, 1982/ (Section 4.2).

4.1 Extrapolation method

In this method the surface acidity constants are determined by extrapolation of the apparent equilibrium constants to zero inner surface charge. The apparent equilibrium constants are calculated from the difference in the amount of acid and base added and the measured concentration in the bulk, $\Delta[H^+]$, the total surface site concentration, the electrolyte concentrations and the K_{A^-} and K_{X+}.

The derivation of the equations used is outlined in the section below. The equations used for calculating ΔH^+ are summarized in Section 4.1.3. The inner surface charge is calculated directly from ΔH^+, as described in Section 4.1.5.

4.1.1 Calculating the apparent equilibrium constants

The apparent equilibrium constants,

$$K_{a1}^{app} = \frac{\{\equiv SOH\}\{H^+_{bulk}\}}{\{\equiv SOH_2^+\}} \qquad [4\text{-}1]$$

$$K_{a2}^{app} = \frac{\{\equiv SO^-\}\{H^+_{bulk}\}}{\{\equiv SOH\}} \qquad [4\text{-}2]$$

can be calculated from the titrations using a number of assumptions outlined below. The first assumption is that the measured difference $\Delta[H^+]$ is only due to the reactions at the inner surface (i.e. the increase or decrease in concentration due to the double layer is assumed negligible.)

$$\Delta[H^+] = [\equiv SOH_2^+] + [\equiv SOH_2^+ A^-] - [\equiv SO^-] - [\equiv SO^- X^+] \qquad [4\text{-}3]$$

To be able to calculate the concentration of $\equiv SOH_2^+$ or $\equiv SO^-$ one has to assume that either the positive or negative sites dominate, i.e.:

at $pH < pH_{pzc}$:

$$\Delta[H^+] = [\equiv SOH_2^+] + [\equiv SOH_2^+ A^-] = [SOH_2^+](1 + K^{int}_{A^-}\{A^-\}) \qquad [4\text{-}4]$$

and at pH > pH_{pzc}:

$$\Delta[H^+] = -([\equiv SO^-] + [\equiv SO^-X^+]) = -[\equiv SO^-](1 + K^{int}_{X+}\{X^+\}) \qquad [4\text{-}5]$$

The mass balance for the total number of surface hydroxyl sites, $[\equiv SOH_{tot}]$:

$$[\equiv SOH_{tot}] = [\equiv SOH_2^+] + [\equiv SOH_2^+ A^-] + [\equiv SO^-] + [\equiv SO^-X^+] + [\equiv SOH] \qquad [4\text{-}6]$$

combined with the [4-4] and [4-5] gives:

$$[\equiv SOH] = [\equiv SOH_{tot}] - \Delta[H^+] \qquad \text{at pH} < pH_{pzc} \qquad [4\text{-}7]$$

and

$$[\equiv SOH] = [\equiv SOH_{tot}] + \Delta[H^+] \qquad \text{at pH} > pH_{pzc} \qquad [4\text{-}8]$$

The apparent equilibrium constants, K_{a1}^{app} and K_{a2}^{app} can be calculated at each pH from:

$$K_{a1}^{app} = \frac{([\equiv SOH_{tot}] - \Delta[H^+])\{H^+_{bulk}\}(1 + K^{int}_{A-}\{A^-\})}{\Delta[H^+]} \qquad [4\text{-}9]$$

$$K_{a2}^{app} = \frac{-\Delta[H^+]\{H^+_{bulk}\}}{(1 + K^{int}_{X+}\{X^+\})([\equiv SOH_{tot}] + \Delta[H^+])} \qquad [4\text{-}10]$$

if the concentrations of the electrolyte at the surface are assumed to be the same as in the bulk. The determination of the ingoing parameters, K_{A-}, K_{X+}, $\Delta[H^+]$ and $[\equiv SOH_{tot}]$ are described in the sections below.

4.1.2 K_{A^-} and K_{X^+}

The K_{A^-} and K_{X^+} can be determined by varying these, minimizing the difference between the different K^{int} for varying ionic strengths. The values of these constants can also be determined by sorption experiments, studying the sorption as a function of pH and ionic strength as was done by /Rundberg, Albinsson and Vannerberg, 1994/ and / Sprycha, 1989: b/ using ^{22}Na and ^{36}Cl as tracers. (see Table 4-1.)

Table 4-1. The intrinsic constants for the ion-pair formation

pK_{Na^+}	pK_{Cl^-}	Material	Reference
-1.2		goethite	/Rundberg, Albinsson and Vannerberg, 1994/
≤-1.6 ϒ	≤-1.5 ϒ	alumina	/Sprycha, 1989: b/

ϒ The values reported by Sprycha were recalculated from the relationships:

$$\equiv SOH_2^+ A^- \leftrightarrow \equiv SOH + H^+ + A^- \quad {}^*K_{A^-}^{int} = \frac{(\equiv SOH)\{A^-\}\{H^+\}}{(\equiv SOH_2^+ A^-)} = \frac{K_{a1}^{int}}{K_{A^-}^{int}}$$

$$\equiv SOH + C^+ \leftrightarrow \equiv SO^-C^+ + H^+ \quad {}^*K_{X^+}^{int} = \frac{(\equiv SO^- X^+)\{H^+\}}{(\equiv SOH)\{X^+\}} = K_{X^+}^{int} \cdot K_{a2}^{int}$$

From these and the determined constants for the protolysis of the surface the general constants for the ion-pair formation can be calculated:

$$pK_{A^-}^{int} = pK_{a1}^{int} - p^*K_{A^-}^{int} = 6.0 - 7.5 = -1.5$$

$$pK_{X^+}^{int} = p^*K_{X^+}^{int} - pK_{a2}^{int} = 8.6 - 10.2 = -1.6$$

Since the reactions are ion-pair formation reactions they should not be dependent on the mineral but only on the effective potential and should be applicable to other minerals as well.

4.1.3 The equations used to calculate $\Delta[H^+]$ from the titration

The $\Delta [H^+]$ is calculated directly from the titrations by:

$$\Delta\left[H^+\right] = \left[H^+_{add}\right] - \left[OH^-_{add}\right] - \left(\left[H^+_{bulk}\right] - \left[OH^-_{bulk}\right]\right) \qquad [4\text{-}11]$$

A massbalance for the actual concentrations of H^+ and OH^- in the aqueous solution of the strong acid and base gives:

$$\left[H^+_{add}\right] = \frac{v_a c_a - v_b c_b}{v_{tot}} + \left[OH^-_{add}\right] = \frac{v_a c_a - v_b c_b}{v_{tot}} + \frac{Q_w}{\left[H^+_{add}\right]} \qquad [4\text{-}12]$$

where v_a, and v_b are the volumes of acid and base added, c_a and c_b are the concentrations of acid and base and Q_w is the water ionization product. Solving above for the H^+ concentration gives:

$$\left[H^+_{add}\right] = \frac{\frac{v_a c_a - v_b c_b}{v_{tot}} \pm \sqrt{\left(\frac{v_a c_a - v_b c_b}{v_{tot}}\right)^2 + 4Q_w}}{2} \qquad [4\text{-}13]$$

(The OH^- concentration is found by reversing the signs.)

The concentration in the bulk is found from the measured potential:

$$\left[H^+_{bulk}\right] = e^{\left(\frac{F}{RT\eta}\left(E - E_0 + \Psi_{H^+} e^{\frac{F}{RT\eta}(E-E_0)}\right)\right)} \qquad [4\text{-}14]$$

4.1.4 The concentration of reactive sites

The concentration of the total number of sites is determined from the site density, N_s (sites / nm^2), the mass concentration, m / V (g/l) and the surface area per unit mass, S_m (m^2 / g):

$$\left[\equiv SOH_{tot}\right] = N_s \frac{m}{V} S_m \frac{1000}{N_A} 10^{18} \qquad [M] \qquad [4\text{-}15]$$

The reported values of the site density range between 2-20 sites / nm^2 /Hayes , Reddem, Ela and Leckie, 1991/. /Rustad, Felmy and Hay, 1996/ calculated the site density on a goethite surface from a molecular statistic calculation for crystals dominated by (110) and (021) crystal faces to be 15-16 sites / nm^2. They found that nearly all surface oxide ions were reactive (19 out of 26 surface sites investigated had a pK^{int} between 7.7 and 9.4). This corresponds to a site density of 11-12 sites/ nm^2. Another way of determining the number of exchangeable sites is by tritium exchange. /Yates, 1975/ used this method to determine the site density of TiO_2 to 12 sites / nm^2. The surface area was measured with BET.

4.1.5 The inner surface charge:

The inner surface charge, σ_0, is calculated from:

$$\sigma_0 = \frac{\left(\left[\equiv SOH_2^+\right] + \left[\equiv SOH_2^+ Cl^-\right] - \left(\left[\equiv SO^-\right] + \left[\equiv SO^- Na^+\right]\right)\right)F}{S_V} = \frac{\Delta[H^+]F}{S_V} \left(C/m^2\right) \qquad [4\text{-}16]$$

where S_V is the surface area per volume (m^2/l).

4.1.6 Limits in the determination of the apparent equilibrium constants

There is a limit to how close to the pH_{pzc} the apparent equilibrium constants can be calculated. As the absolute value of the surface charge decreases the difference between the number of positive and negative sites will decrease. Thus the assumption that one of the two will dominate does not hold:

$$\lim_{\Delta[H+]\to 0} K_{a1}^{app} = \lim_{\Delta[H+]\to 0} \frac{\left([\equiv SOH_{tot}] - \Delta[H^+]\right)\left\{H_{bulk}^+\right\}\left(1 + K_{A^-}^{\text{int}}\{A^-\}\right)}{\Delta[H^+]} \to \infty \quad [4\text{-}17]$$

and

$$\lim_{\Delta[H+]\to 0} K_{a2}^{app} = \lim_{\Delta[H+]\to 0} \frac{-\Delta[H^+]\left\{H_{bulk}^+\right\}}{\left(1 + K_{X+}^{\text{int}}\{X^+\}\right)([\equiv SOH_{tot}] + \Delta[H^+])} = 0 \quad [4\text{-}18]$$

and thus

$$\lim_{\Delta[H+]\to 0} pK_{a1}^{app} \to -\infty \quad [4\text{-}19]$$

$$\lim_{\Delta[H+]\to 0} pK_{a2}^{app} \to \infty \quad [4\text{-}20]$$

The effect of this can be seen by plotting pK^{app} vs. σ_0 (see Figure 6.4 Section 6). The pK^{app} will level off and then asymptotically tend towards positive and negative infinity. Due to this care has to be taken in the choice of data points used in the extrapolation, excluding the ones too close to pH_{pzc}.

A preliminary investigation of which factors that affect the determination of the acidity constants indicate that the site density and the values of the outer sphere complexation constants with the supporting electrolyte have the largest impact on the resulting acidity constants. In determining the capacitance the base concentration and the site density are of the largest importance.

4.2 Determining K_{a1} and K_{a2} using FITEQL

The program FITEQL /Westall, 1982/ was used to determine the constants in one titration. The program finds the best fit using least squares. The in data to the program is the pH, the measured $\Delta[H^+]$, the model used, the capacitances used in the model, the surface area, concentration of solid and the ionic strength. The four different models available in the program have been used, Constant Capacitance Model (CCM), Stern model, Diffuse Layer Model (DLM) and Triple Layer Model (TLM).

5 Experimental

5.1 Reagents and reagent preparations

All chemicals were reagent grade. All solutions were made with MilliQ-water.

NaOH: To reduce the amount of carbonate present in the base, $Ba(NO_3)_2$ was added to a ≥10 M base solution. This solution was filtered and diluted as needed. The concentration was determined by the calibration titration (see Section 3). The base was stored in a CO_2-free atmosphere. (The resulting concentration of Ba in the experiments from the base was lower than $2 \cdot 10^{-9}$ M.)

TiO_2 : Degussa P-25. Titrations were performed both on TiO_2 in its original form and on washed TiO_2. The TiO_2 was washed at least 10 times with MilliQ-water. The conductivity of the supernatant after centrifugation at 10,000 rpm for 30 minutes decreased from ca 140 to 18 μS. The surface area of the TiO_2 was measured by BET(N_2) and determined to 49.9 ± 0.2 m^2/g. Nitrogen tends to adsorb only on external surfaces (≡SOH type) of phyllosilicate minerals and oxides. Therefore the area obtained by BET using N_2 should be representative for the surface hydroxyl groups /Bradbury and Bayens, 1993/.

Alumina: The alumina was a neutral aluminum oxide powder from JT Baker; its surface area was determined with multipoint BET to 142.9 m^2/g. The alumina was not pretreated.

^{234}Th: ^{234}Th was used as a tracer, extracted from a solution of depleted uranium /Albinsson and Ekberg, 1998/. The total concentration of Th was determined by ICP-MS for each batch of Th prepared.

^{60}Co: NEN, DuPont. To remove any impurities of iron from the solution the pH of the stock solution was increased to about 5, the solution was centrifuged for 30 minutes at 19,000 g, and the supernatant was used.

^{237}Np: A 0.5 M stock solution of ^{237}Np was prepared by dissolving neptunium oxide in perchloric acid. A secondary stock solution was prepared by diluting with deionized water to 5×10^{-4} M. The pH of the solution was adjusted to 4, the solution was centrifuged at 19,000 g for 30 minutes and the supernatant was used.

U(VI) solution: The ^{232}U solution was provided by LANL (produced by neutron capture in ^{231}Pa). The ^{232}U solution was separated from its daughters by means of an anionic exchanger before the sorption experiments. A >99.92% pure solution of natural uranium from JT Baker was used for sorption at higher concentrations.

Nitrogen: The gas was passed through a 1 M NaOH solution and MilliQ-water before

entering the setup to reduce the presence of carbonate.

5.2 Titrations

5.2.1 Titrations of TiO_2

All titrations of the TiO_2 were carried out in a temperature controlled plastic vessel at 25°C under nitrogen atmosphere. The automatic titration unit consisted of a Radiometer titrator, ABU91, and a program controlling the titrations (size and time interval for the additions). Prior to all the titrations the solution and solid were acidified by addition of a known amount of acid and purged by nitrogen for at least 1 h to remove CO_2.

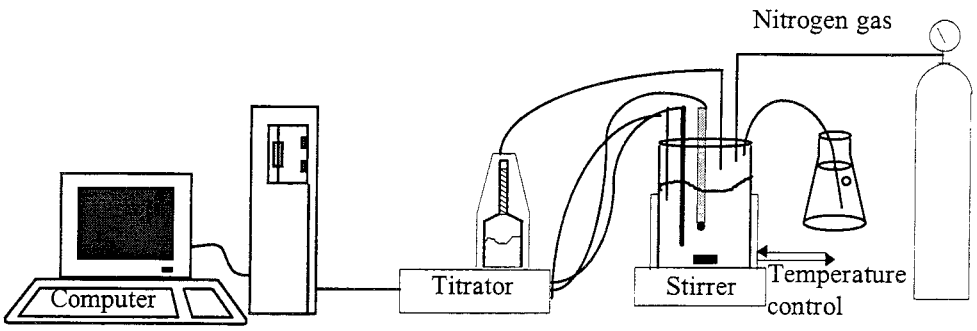

Figure 5.1 *The titrator setup.*

/Carlsson, 1994/ observed a hysterisis in titrating a solution from the acid side to the base and back again and conducted all his titrations from the original pH to the base or acid side. A few back titrations were made to study the hysterisis. Before each titration a calibration titration without the solid was made in the same manner. The pH was measured with a glass electrode (Radiometer, PHG201) and an open junction reference electrode (Radiometer, K102-K).

The time between each step in the titration should be long enough for equilibrium to be reached throughout the solution but not too long for two reasons: i) a two step kinetics has been observed on the base side by both (Janssen and Stein, 1986/ and /Bérubé and Bruyn, 1968/. Bérubé and Bruyn concluded that this second step could not be due to proton diffusion by measuring tritium consumption. Janssen and Stein attributed this to contamination of CO_2 on the TiO_2 surface already present affecting the sorption and therefore extrapolated to time zero. ii) The acid or base will diffuse from the byrette tip changing the actual concentration. Fifteen minutes between the additions was chosen. The kinetics of the titrations can be followed as a program records a number of measurements (determined by the user) as a function of time for each addition. At each

point of measurement a number of readings (also specified by the user) are made from which the average and standard deviation are calculated.

A number of titrations at different electrolyte concentrations (0.005-0.1 M Na(Cl, ClO_4)) were performed. The electrolyte concentration in each titration did not vary more than 2 %. The base was added in sizes of 10 - 100 µl to a 100 ml solution. At low solid concentrations the uncertainty in the determination of the difference in H^+ becomes very large. At high concentrations there is the risk of an inhomogenous suspension and of a suspension effect in measuring the pH. Commonly titrations are performed at concentrations around 2 - 20 g/l. Most of the titrations were carried out at a concentration of about 10 g/l.

If there are no reversibly bound impurities on the surface the pH of a solution with the solid will approach the pH_{pzc} asymptotically as the solid to liquid ratio is increased /Noh and Schwarz, 1989/. The pH of a highly concentrated solution, the so called pH_∞ was measured as well for comparison. The concentration needed was determined by a so called mass titration, adding solid until the pH did not alter any more.

5.2.2 Titrations of alumina

The titrations of the alumina surface were carried out in principle in the same manner as for the TiO_2. All titrations were carried out in a temperature controlled glass beaker at 25°C under argon atmosphere at different electrolyte concentrations (0.01 - 1 M $NaNO_3$). The automatic titration unit consisted of a Hamilton injection dispenser, a Keithley 617 Electrometer and a LABVIEW program for measuring the potential and controlling the titrations (size and time interval for the additions), developed by /Rundberg 1996/. Prior to all titrations the solution and solid were mixed, a specific amount of acid added and the solution was purged by argon for at least 1h to remove CO_2. For each ionic strength a Gran calibration titration without the solid was made in the same manner. The pH was measured with a combination glass electrode with a Ross reference sleeve junction for NaCl titrations. By using a double junction reference electrode with the same outer solution as the one titrated, the influence of diffusion was minimized. Additions were made in intervals of 15 min. for the calibration titrations and 2 hr. for the surface titrations. It was estimated that equilibrium was reached to at least 98 % for these time intervals. One back titration was made for 1 M $NaNO_3$.

Studies of the dissolution of alumina as a function of pH were performed since dissolution of the surface can affect the sorption by decreasing or increasing the number of sites available. The total concentration of Al in the aqueous phase was measured as a function of pH. A mixture of 0.1 g solid and 10 ml NaCl solution in Beckman centrifuge tubes was separated by centrifugation at 30,000 g for 30 minutes. The total concentration of Al in the aqueous phase was measured after separation /Sherif 1998/. The pH was measured after separation with a combination electrode calibrated with a Gran titration.

5.3 Sorption studies

The sorption was calculated from measurements of the radioactivity of the nuclides in the phases (directly or indirectly) at varying pH and ionic strength. Two different methods were employed; one with individual samples set at different pH and one withdrawing samples from the same mixture at varying pH.

1. Batch sorption
The batch sorption was performed in centrifuge tubes at room temperature. All handling of the samples except centrifugation was made in a glove box with nitrogen atmosphere. To each tube the solid, the electrolyte solution, acid or base and stock solution were added in that order. After two days of equilibrium time the liquid was separated from the solid by means centrifugation. Two samples of the aqueous phase were taken; one for pH measurements and one for determining the concentration of the radionuclide in the aqueous phase. Reference samples at different pH's were made for each series. For practical reasons the pH was measured with a combination electrode.

2. Samples from the same solution
The sorption was studied by withdrawing samples, at various pH, from the same solution. The solid and the electrolyte were mixed in a glass vessel under nitrogen atmosphere, acid was added and the solution was stirred before the stock solution was added. The pH was measured with the same setup as was used in the titrations. After an addition of acid, more than 5 minutes were allowed to pass before the sample was withdrawn into centrifuge tubes using a syringe. The rest of the separation was carried out in the same manner as for the batch sorption. (The pH of the aqueous phase after separation was measured in a few of the samples for control purposes.) The desorption was studied by decreasing the pH of the solution.

6 Results

6.1 Results from titrations on TiO_2

Several titrations were performed both on unpurified and purified titanium dioxide. The experimental setup that worked best was with additions made every fifteen minutes after an initial purging of the system for 1 h. All additions were of the same size. Before each titration a Gran calibration was made. As can be seen from the Figures 6.1 to 6.3 portraying the inner surface charge as a function of pH for the different degrees of purified titanium dioxide the cleaner the closer to $\sigma = 0$ the curves of the different ionic strengths will intersect. The curves tend to intersect at a higher pH as the impurities increase. The pH at which the curves intersect is around 6.2, which agrees well with the pH_{pzc} obtained from the calculations. The pH in a concentrated solution (>20g/l) of purified TiO_2 was between 5.74 and 6.05 (pH_∞).

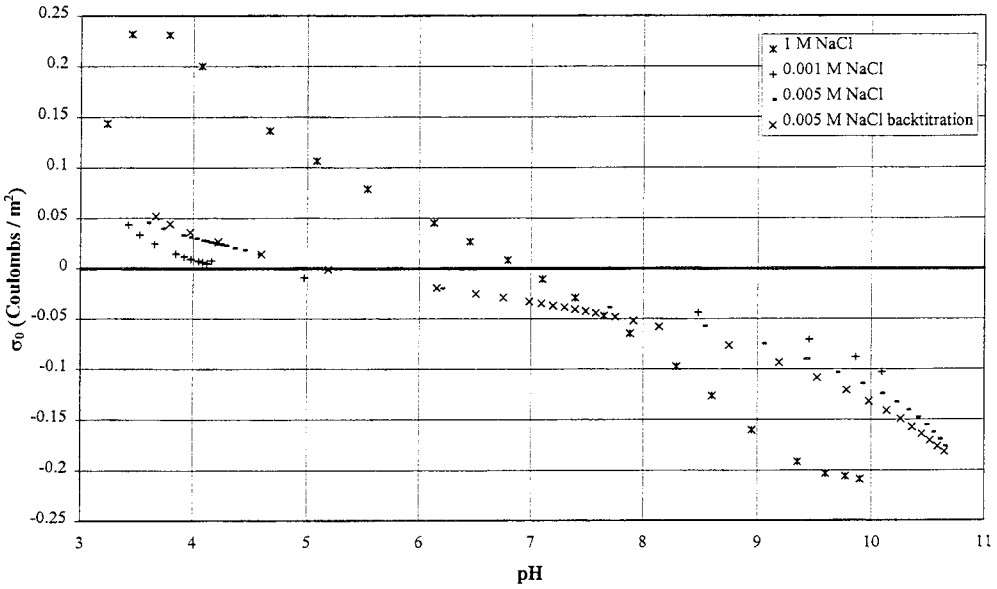

Figure 6.1 *Inner surface charge as a function of pH for unwashed titanium dioxide. Note that the scale on the axis are not the same as Figure 6.2 and 6.3.*

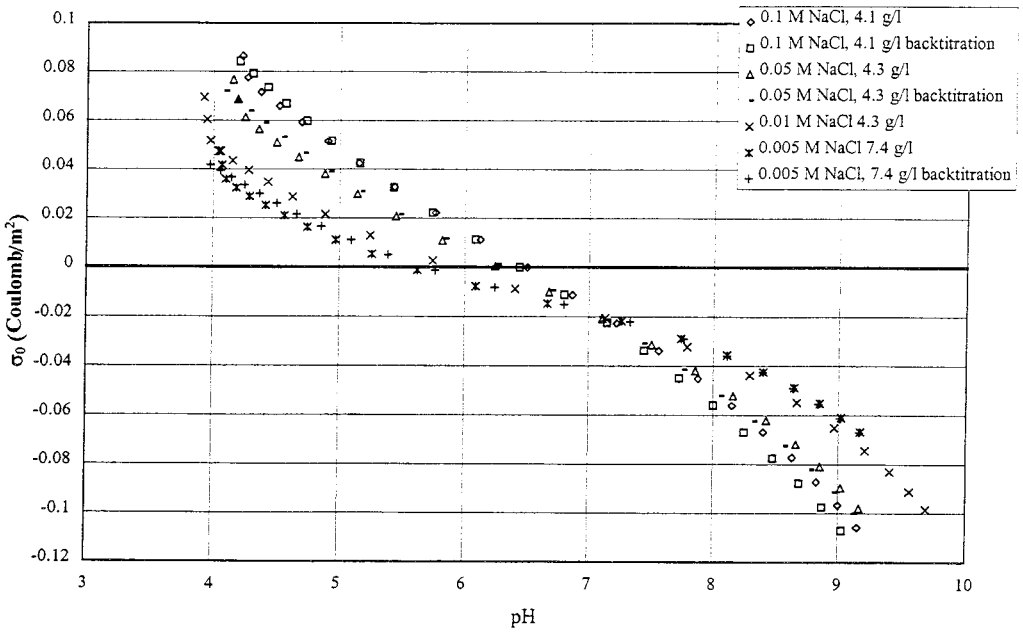

Figure 6.2 *The inner surface charge as a function of pH for washed but not completely purified titanium dioxide.*

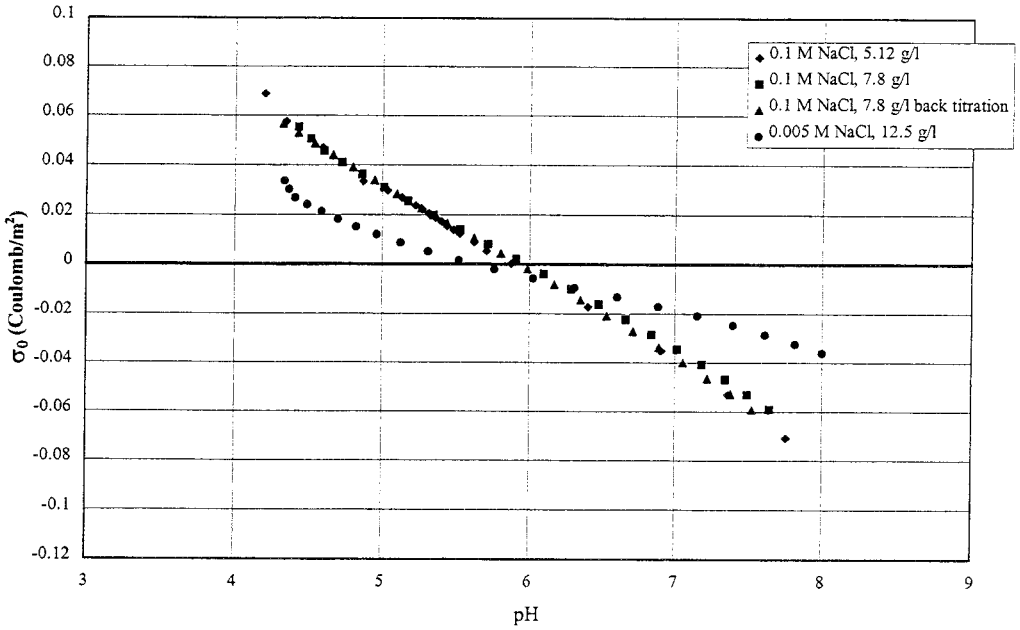

Figure 6.3. *The inner surface charge as a function of pH for purified titanium dioxide.*

The forward and back titrations follow each other nicely, indicating very small hysterisis. This shows that the titrations were good, i.e. there is no (irreversible) alteration of the surface during the titration and the additions are accurate.

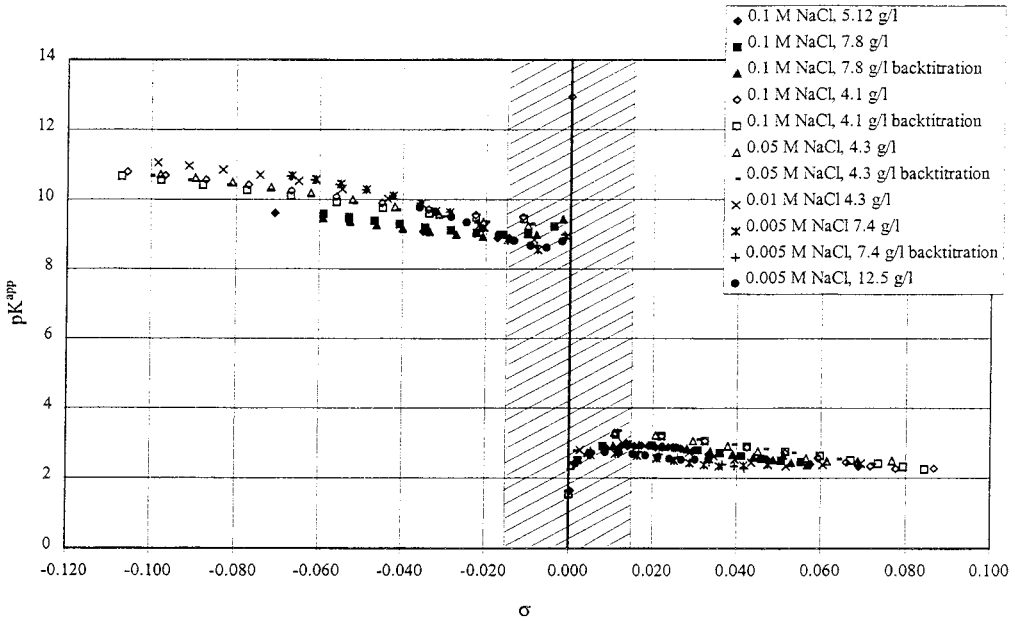

Figure 6.4 *The - log of the apparent equilibrium constant as a function of the inner surface charge. Two different sets of purified titanium dioxide have been used. The results from the purest batch are indicated with the filled symbols.*

As can be seen in Figure 6.4 the pK^{app} for the acid side agree well with each other, independently of the ionic strength. The pK^{app} of the base side do not fall together as well as on the acid side. In Table 6-1 the values of the slopes and resulting capacitances are summarized.

Close to pH_{pzc} the curves tend to curve towards positive and negative infinity as was described in Section 3.1.6. This is due to the assumption that either the positive or negative sites dominate. This assumption does not hold close to pH_{pzc}. In the extrapolation these points have been excluded. Only values with an absolute sigma greater than 0.015 were used (outside the striped region).

In all the calculations the pK_{A^-} and pK_{X^+} used were the ones reported by /Rundberg , Albinsson and Vannerberg, 1994/ for Na on goethite and for Cl^- on alumina by /Sprycha, 1989:b/ (Table 4-1).

Table 6-1. The intrinsic acidity constants, pH_{pzc} and capacitances determined from extrapolation.

Ionic strength (M)	g / L	pK^{int}_{a1}	pK^{int}_{a2}	pH_{pzc}	slope acid side	slope base side	C_1 acid side	C_1 base side	correlation acid side	correlation base side
0.1*	5.11	3.17	8.63	5.90	-12.81	-13.81	1.3	1.2	0.981	0.993
0.1*	7.82	3.21	8.73	5.97	-13.83	-14.30	1.2	1.2	0.994	0.990
0.1 (back)*	7.82	3.24	8.62	5.93	-14.80	-14.19	1.1	1.2	0.987	0.995
0.005*	12.54	2.91	8.30	5.60	-14.18	-41.80	1.2	0.4	0.999	0.998
0.01	4.30	3.26	8.93	6.09	-18.32	-23.12	0.9	0.7	0.993	0.969
0.0055	7.44	2.90	8.73	5.82	-15.85	-30.72	1.1	0.6	0.996	0.973
0.0055 (back)	7.44	3.09	8.65	5.87	-18.95	-32.05	0.9	0.5	0.996	0.973
0.05	4.30	3.60	9.04	6.32	-18.19	-17.93	0.9	0.9	0.999	0.994
0.05(back)	4.30	3.63	9.02	6.32	-16.97	-16.92	1.0	1.0	1.000	0.998
0.1	4.15	3.56	9.22	6.39	-16.09	-15.20	1.1	1.1	0.977	0.998
0.1(back)	4.15	3.54	9.13	6.34	-15.38	-14.52	1.1	1.2	1.000	0.998

* purified titanium dioxide

The resulting values of the constants were calculated to: $pK^{int}_{a1} = 3.5 \pm 0.3$, $pK^{int}_{a2} = 8.9 \pm 0.2$, and $pH_{pzc} = 6.2 \pm 0.4$, by weighing the values from each titration with the variance obtained from the extrapolations.

The capacitance, C_1, was calculated from the slope in the extrapolation:

$$C_1 = \frac{F}{slope\, RT \ln 10} \qquad [6.1\text{-}1]$$

The values are in the right order of magnitude /Hayes, Redden, Ela and Leckie, 1991/. On the base side the capacitance varies more than on the acid side (which can be seen in Figure 6.4 comparing the slopes.) It appears that the ionic strength may affect the capacitance on the base side more than on the acid side.

A further support for the validity of a constant capacitance model (whether CCM, TLM or Stern) describing the solid liquid interface is that the pK^{app} vs. sigma gives a straight line for the pure titanium dioxide, see Fig 6.4.

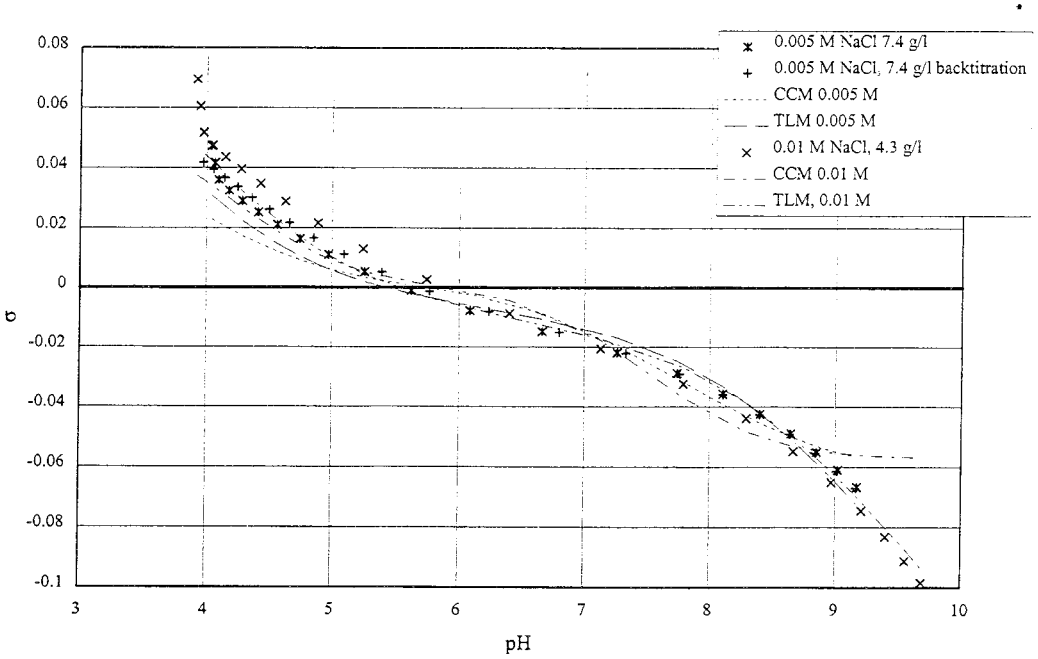

Figure 6.5. *Result from modeling two titrations of two different ionic strengths. The only two models that converged were the constant capacitance model and the triple layer model. The resulting constants are summarized in the table 6-2 below.*

Unfortunately FITEQL was not able to find a solution to the data in the titrations using other models than the constant capacitance and the triple layer model. The resulting constants are summarized in Table 6-2. As can be seen there is a larger spread in the constants between the two models than between the two titrations. The second acidity constants are well below the ones found from the extrapolations and thus the pH_{pzc} is much lower as well (average =5.3).

Table 6-2. The determined constants from the modeling with FITEQL

Model / Ionic strength	pK^{int}_{a1}	pK^{int}_{a2}	pH_{pzc}	pK^{int}_{A-}	pK^{int}_{X+}
CCM /0.01	4.30	7.43	5.87		
TLM[a] /0.01	2.47	6.8	4.64	2.47-4.16=-1.69	6.8-8.64=-1.84
CCM /0.005	4.13	7.32	5.73		
TLM[a] /0.005	2.58	6.99	4.79	2.58-4.37 =-1.79	6.99-8.01=-1.02

[a] since FITEQL would not converge the constants had to be found iteratively, first determining the acid side constants, and from these the base. This set were used twice again to determine the final constants.

In the modeling C_1 was set to 1.2 and C_2 to 0.2. All the other constants were the same as the ones used in the extrapolation.

The values reported in the literature for the pH_{pzc} and the acidity constants vary greatly as can be seen in Table 6-3, depending on the method used.

/Noh and Schwarz, 1989/ studied the same TiO_2 as was used in this work. They found a large discrepancy between the pH_{pzc} and pH_{∞} (4.9 and 4.0 respectively) and attributed this to the possible contamination of Cl. We also found a large effect on the titrations if the TiO_2 was purified or not. The nature of the impurities have not been further investigated, but it is clear that they were easily removable by several washing with

MilliQ water. The pH of a concentrated solution (> 20 g/l) of washed TiO_2 gave a pH of 6. This agrees well with the pH_{pzc} found from the extrapolations. As was described by /Zalac and Kallay, 1992/ any impurities on the mineral oxide will cause a discrepancy between the pH_{pzc} and pH_{∞}.

Table 6-3. Some other literature data on TiO_2:

pK_{a1} / p^*K_{anion}	pK_{a2} / p^*K_{cation}	pH_{pzc}	method	reference
		6.0 ± 0.2	calorimetric titration of rutile suspension	/Machesky and Anderson, 1986/
3	9	6	zeta potential	/Sprycha, 1986/
3.0 / 4.8	8.6 / 6.8	5.8	potentiometric titration, KNO_3	/James, Stiglich, and Healy, 1981/
	9.3 - 10.0	~7.1	titration, double extrapolation	/Carlsson , 1994/
		5.9	zeta potential	/Wiese and Healy, 1975/
		5.21	modeling from crystal data and Born solvation	/Sverjensky, 1994/
		pH_{iep}: 6.5 pH_{pzc}: 4.9± 0.5 pH_{∞}: 4.0	pH stat, zeta potential mass titration	/Janssen and Stein, 1986/ /Noh and Schwarz, 1989/
3.5± 0.3/ 5.0*	8.9±0.2/ 10.1*	6.2 ± 0.4	potentiometric titrations, extrapolation	this study
3.4 /4.3	7.1 / 8.3	5.3	potentiometric titrations, modeling with FITEQL	this study
		6	mass titration, pH in concentrated solution	this study

* the p^*K_{X+} and p^*K_{A-} are calculated using the values reported in Table 4-1.

It is interesting to note that modeling from a thermodynamic point of view yields quite good agreement with the observed values of the pH_{pzc}. Sverjensky [SVE 94]. predicted the point of zero charge to be 5.21 from crystal chemistry and solvation theory. He found a dependence on the dielectric constant and the Pauling electrostatic bond strength and was able to predict the surface protonation reactions from only the underlying crystal which implies a similarity of the proton bonding more to the bulk crystal than to the aqueous complexes.

6.2 Results from titrations on alumina

The intrinsic equilibrium constants for the surface acidity reactions were determined to $pK_{a1}^{int} = 7.0 \pm 0.5$, $pK_{a2}^{int} = 11.6 \pm 0.3$ from the titrations by extrapolating the apparent equilibrium constants, K_{a1}^{app} and K_{a2}^{app}, to zero inner surface charge (Figure 6.6).

As for the titanium dioxide the data close to zero inner surface charge were not used in the extrapolation. The pK_{cation} used was the same as for the titanium dioxide. However we found no value for the pK_{NO3}. If this parameter was used as a fitting parameter the value of the constant became 1. This value was used.

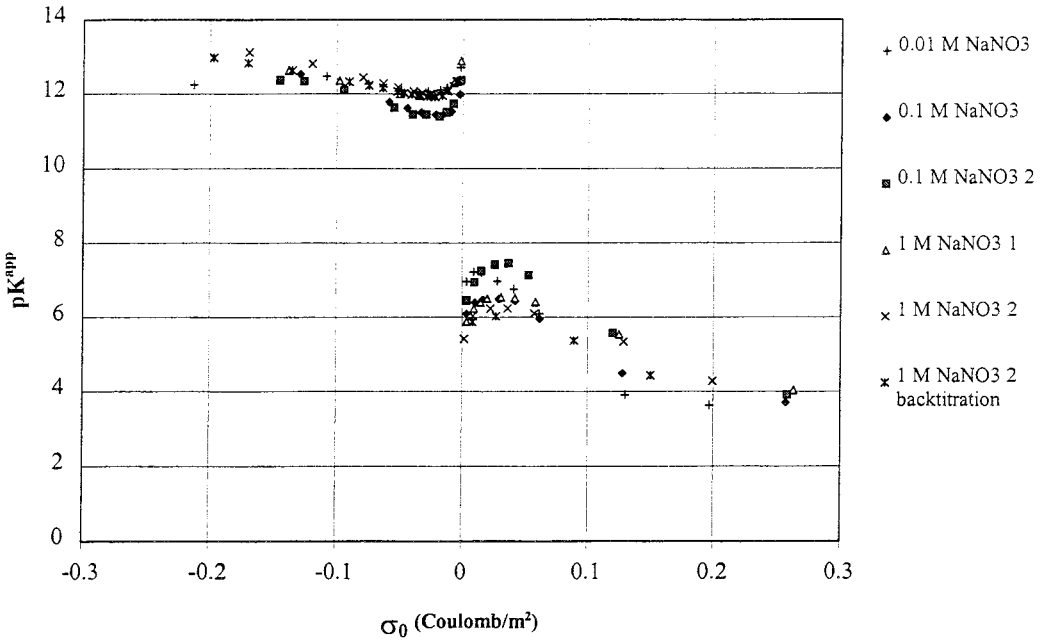

Figure 6.6 *The negative log of the apparent equilibrium constants as a function of surface charge of the alumina.*

Table 6-4. The intrinsic acidity constants, pH_{pzc} and capacitances determined from extrapolation.

Ionic strength (M)	g / L	pK^{int}_{a1}	pK^{int}_{a2}	pH_{pzc}	slope acid side	slope base side	C_1 acid side	C_1 base side	correlation acid side	correlation base side
0.10	9.92	6.68	11.31	9.00	-12.75	-9.86	1.3	1.7	0.928	0.988
0.10	9.94	7.70	11.34	9.52	-15.29	-8.12	1.1	2.1	0.969	0.953
1.00	9.48	7.06	11.86	9.46	-10.82	-6.00	1.6	2.8	0.988	0.970
1.00	9.88	6.82	11.85	9.33	-11.37	-8.53	1.5	2.0	0.975	0.985
1.00	9.88	6.60	11.83	9.21	-13.05	-6.36	1.3	2.7	0.989	0.998
0.01	10.08	7.41	12.02	9.72	-21.90	-4.63	0.8	3.7	0.938	0.886

There is a large deviation in the capacitances on the base side.

Table 6-5. Some other literature data on Al_2O_3:

pK_{a1} / p^*K_{anion}	pK_{a2} / p^*K_{cation}	pH_{pzc}	method	Reference
5.6/7.1	11.6/10.2	8.6	potentiometric titration	/Zhang, Sparks and Scrivner, 1994/
5.0	11.25		zeta potential	/Sprycha 1989:a/
4.9	11.3		potentiometric titration	/Sprycha, 1989:b/
≥6.0/7.5	≤10.2/8.6	8.1	adsorption measurement	/Sprycha, 1989:b/
7.9	9.22	8.6	not specified in text	/Marmier, Dumonceau, Chupeau and Fromage, 1994/
7.0/8.3	8.8/8.3		potentiometric titration, fitted with FITEQL	/Toner and Sparks, 1995/
7.9	9.1	8.5	potentiometric titration	/Huang and Stumm, 1973/

The dissolution of alumina was studied as a function of pH and time. As can be seen in Figure 6.7 the dissolution is lower than the equilibrium concentration after a time period of two days which was the longest time for the sorption experiments.

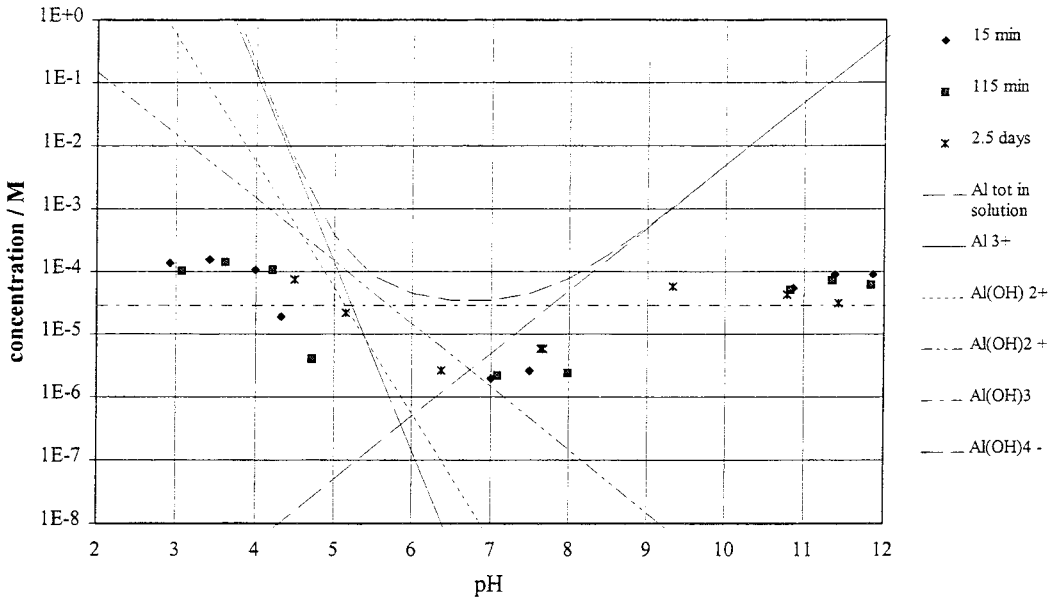

Figure 6.7. *The dissolution of alumina in 0.1 M NaCl as a function of pH. The speciation refers to the concentrations of Al in a solution saturated with respect to alumina.*

The concentration of dissolved alumina in a solution of lower total concentration of alumina is not likely to be higher during the same time interval studied. Assuming that the concentration of dissolved alumina will be the same in a solution with 0.5 g alumina / L the % dissolved will not exceed 1.3 %

6.3 Results from sorption studies

The reactions and constants used for evaluation of the sorption results onto TiO_2 are summarized in Table 6-6.

Table 6-6. Reactions and constants for Np, Co and Th

Reaction	Constant	Reference
Acid dissociation of titanium dioxidide surface:		
$SOH + H^+ \Leftrightarrow SOH_2^+$	$pK_{a1}^{int} = 3.1$	
$SOH \Leftrightarrow SO^- + H^+$	$pK_{a2}^{int} = 8.5$	
$SOH_2^+ + Cl^- \Leftrightarrow SOH_2^+ Cl^-$	$pK_{Cl^-}^{int} = 1.5$	/Sprycha 1989:b/
$SO^- + Na^+ \Leftrightarrow SO^- Na^+$	$pK_{Na^+}^{int}=1.2$	/Rundberg, Albinsson and Vannerberg, 1994/
Aqueous cobalt speciation		
$Co^{2+} + H_2O \Leftrightarrow Co(OH)^+ + H^+$	$pK_{Co1}=9.65$	/Baes and Mesmer, 1986/
$Co^{2+} + 2\ H_2O \Leftrightarrow Co(OH)_2 + 2H^+$	$pK_{Co2}=18.8$	/Baes and Mesmer, 1986/
$Co^{2+} + 3\ H_2O \Leftrightarrow Co(OH)_3^- + 3H^+$	$pK_{Co3}=31.5$	/Baes and Mesmer, 1986/
$Co^{2+} + 4\ H_2O \Leftrightarrow Co(OH)_4^{2-} + 4H^+$	$pK_{Co4}=46.3$	/Baes and Mesmer, 1986/
Aqueous neptunyl speciation		
$NpO_2^+ + H_2O \Leftrightarrow NpO_2(OH) + H^+$	$pK_{NpO2\text{-}1}=8.9; 11.7$	/Allard, Kipatsi, and Liljenzin, 1980/; /Lierse, Treiber, Kim, 1985/
$NpO_2^+ + 2\ H_2O \Leftrightarrow NpO_2(OH)_2^- + 2H^+$	$pK_{NpO2\text{-}2}=17.8; 23.1$	/Allard, Kipatsi, and Liljenzin, 1980/; /Lierse, Treiber, Kim, 1985/
Aqueous thorium speciation		
$Th^{4+} + H_2O \Leftrightarrow Th(OH)^{3+} + H^+$	$pK_{Th1}=3.8$	/Baes and Mesmer, 1986/
$Th^{4+} + 2\ H_2O \Leftrightarrow Th(OH)_2^{2+} + 2H^+$	$pK_{Th2}=7.7$	/Baes and Mesmer, 1986/
$Th^{4+} + 3\ H_2O \Leftrightarrow Th(OH)_3^{+} + 3H^+$	$pK_{Th3}=12.7$	/Baes and Mesmer, 1986/
$Th^{4+} + 4\ H_2O \Leftrightarrow Th(OH)_4 + 4H^+$	$pK_{Th4}=16.9$	/Baes and Mesmer, 1986/
$2Th^{4+} + 2\ H_2O \Leftrightarrow Th_2(OH)_2^{6+} + 2H^+$	$pK_{Th2\text{-}2}=6.14$	/Baes and Mesmer, 1986/

Inner layer capacitance:	1.2 C/m^2	Site density*:	12 sites / nm^2
Outer layer capacitance	0.2 C/m^2	pKw:	13.8
Surface area (BET):	50 m^2/g	I:	0.1 M

* The surface site density used is from measurements made by Yates on TiO_2 using tritium exchange. /Yates, 1975/

Neptunyl sorption onto TiO_2

The results from the sorption of neptunyl as a function of pH and ionic strength along with the results from the fitting of the data are shown in Figure 6.8.

Only data which are below the detection limit were included in the fitting of the reactions to the data using FITEQL. The resulting reactions from the fitting have been modeled over a wider pH range to predict the sorption at higher pH.

Observations:

1. The lack of ionic strength dependence indicates the formation of an inner-sphere complex with the surface.
2. A decrease in pH from 10 to 2.5 gave decrease in sorption from $K_d > 10^5$ to

~20 indicating that the reaction is reversible.
3. The slope of relationship between log K_d and pH is unity thus one proton is released in the reaction.

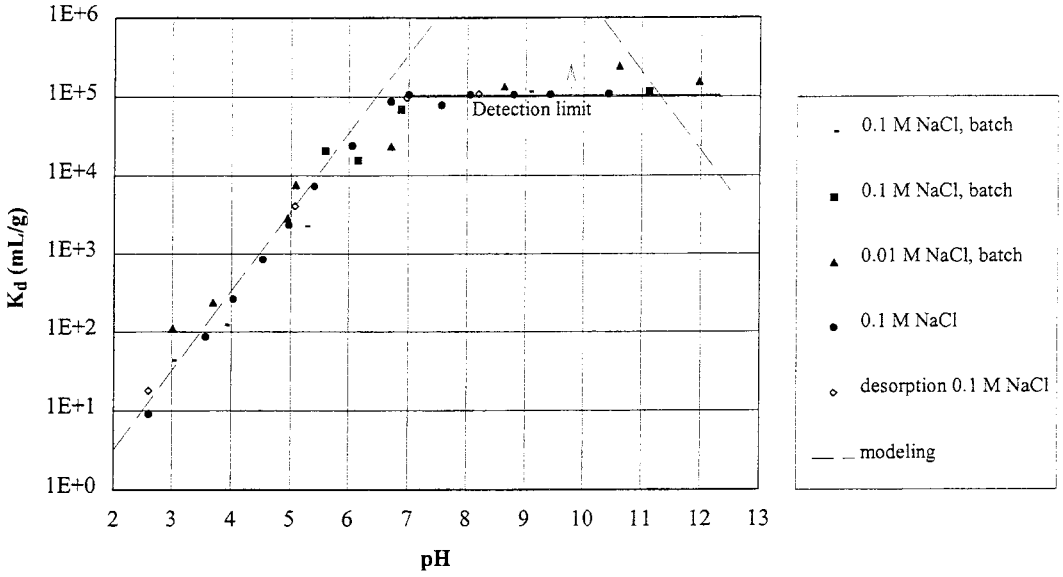

Figure 6.8 *The Np sorption onto TiO_2 as a function of pH at various ionic strengths; both batch wise and on-line sorption experiments. Concentration of Np is $2.5x10^{-5}$ M. Above pH 7 the detection limit is reached for the concentration that can be determined in the aqueous phase, indicated by the arrow.*

Reaction
Thus neptunyl forms a neutral inner-sphere complex with the TiO_2 which can be described by the reaction

$$\equiv SOH + NpO_2^+ \xleftrightarrow{K} \equiv SONpO_2 + H^+ \qquad K = 10^{-1.5} \qquad [6.2\text{-}1]$$

Cobalt sorption onto TiO_2

The results from the sorption of Co are presented both as log K_d vs. pH (Fig. 6.9) and as % sorbed vs. pH (Fig 6.10).

Observations:

1. The lack of ionic strength dependence indicates the formation of an inner-sphere complex with the surface.
2. A decrease in pH from 10 to 5 gave decrease in sorption from $K_d > 10^5$ to ~ 40 indicating that the reaction is reversible at least to pH 5. (Below this point the reaction might be reversible if more time is allowed to pass.)
3. The slope of relationship between log K_d and pH is ~1.5.

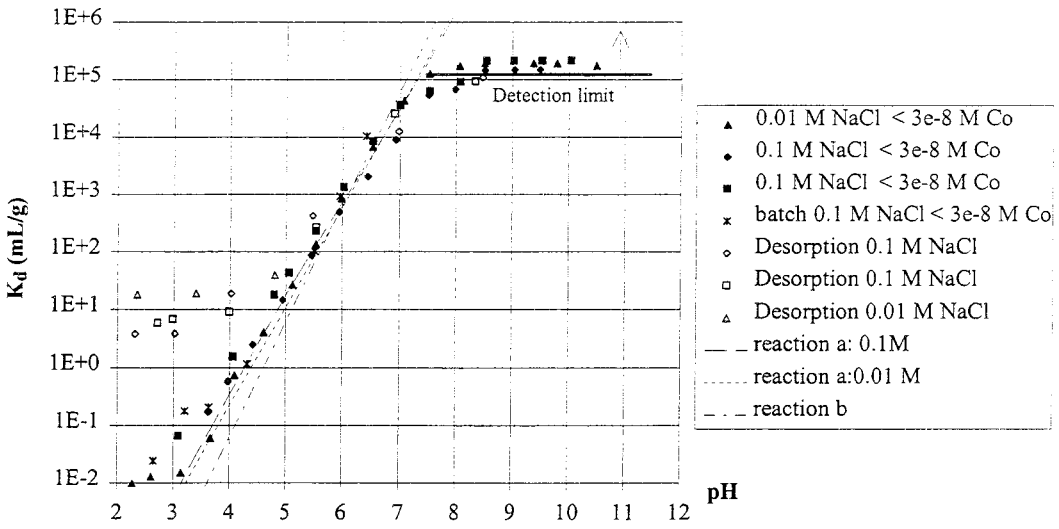

Figure 6.9 *The cobalt sorption as a function of pH and ionic strength. Two different modeled reactions are shown; forming a positive complex releasing one proton (reaction a) and forming a neutral complex releasing two protons (reaction b).*

Reaction:

Different reactions were tried in order to fit the cobalt sorption data. The reaction that gave the best fit to the data (the best goodness of fit as defined in FITEQL /Westall, 1982/ was the formation of a positively charged complex, releasing one proton (reaction a in Figure 6.9). The reaction can either be expressed as formation of a complex with the first hydrolysed species:

$$\equiv SOH + Co^{2+} + H_2O \longleftrightarrow \equiv SOHCo(OH)^{+} + H^{+} \qquad [6.2\text{-}2]$$

or with the loss of a proton from the surface hydroxyl group:

$$\equiv SOH + Co^{2+} \overset{K}{\longleftrightarrow} \equiv SOCo^{+} + H^{+} \qquad K = 10^{-3.4} \qquad [6.2\text{-}3]$$

Since the stoichiometry of these reactions is the same except for the water, the model can not distinguish between them. In addition an outer sphere complex with the supporting electrolyte is formed:

$$\equiv SOH + Co^{2+} + A^{-} \overset{K}{\longleftrightarrow} \equiv SOCo^{+} - A^{-} + H^{+} \quad K = 10^{-2.6} \qquad [6.2\text{-}4]$$

The equilibrium constant for this reaction can be expressed as:

$$K^{\text{int}} = \frac{\left[\equiv SOHCo(OH)^{+}\right]\left[H^{+}\right]_{bulk} e^{\frac{-F\Psi_0}{RT}}}{\left[\equiv SOH\right]\left[Co^{2+}\right]_{bulk} e^{\frac{-2F\Psi_0}{RT}}} = K^{app} e^{\frac{F\Psi_0}{RT}} \qquad [6.2\text{-}5]$$

where K^{int} is the intrinsic equilibrium constant (referring to the concentrations of the species at the surface), Ψ_0 is the potential difference between the inner surface and the bulk, and $[i]$ is the concentration of species i. From this it can be seen that the apparent equilibrium constant will be dependent on the surface potential:

$$\log K^{app} = \log K^{\text{int}} - \frac{F\Psi_0}{RT\ln 10} \qquad [6.2\text{-}6]$$

Thus the apparent equilibrium constant will be dependent on the pH via the surface potential. This can explain the non-integer slope.

Reaction b is included as a comparison. In this reaction two protons are released as a neutral complex is formed:

$$\equiv \text{SOH} + \text{Co}^{2+} + \text{H}_2\text{O} \longleftrightarrow \equiv \text{SOCo(OH)} + 2\text{H}^{+} \qquad [6.2\text{-}7]$$

This reaction results in a slope of 2 which can be seen in Figure 6-9.

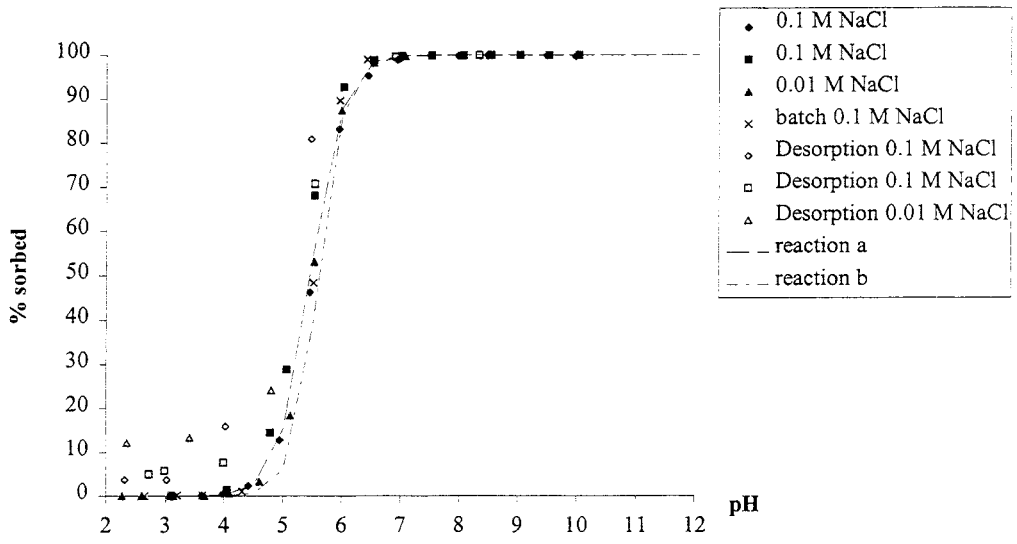

Figure 6.10 *The % of Cobalt sorbed. The data and models are the same as in Figure 6.8*

As can be seen in Figure 6.10 the fraction sorbed vs. pH does not show the difference between the different models as clearly as the K_d vs. pH representation does. Fewer data points are of use and the dependence on the determination of the pH looks larger.

Thorium sorption onto TiO_2

The Th sorption was studied mainly using the batch method. One on-line experiment checking the desorption was performed. The experimental results are presented together with the resulting fit in Figure 6.11.

Observations:

1. The lack of ionic strength dependence indicates the formation of an inner-sphere complex with the surface.
2. A decrease in pH from 2 to 1 decreased the sorption from K_d ~10^4 to ~10 indicates that the reaction is reversible.
3. The slope of relationship between log K_d and pH is ~2.7.

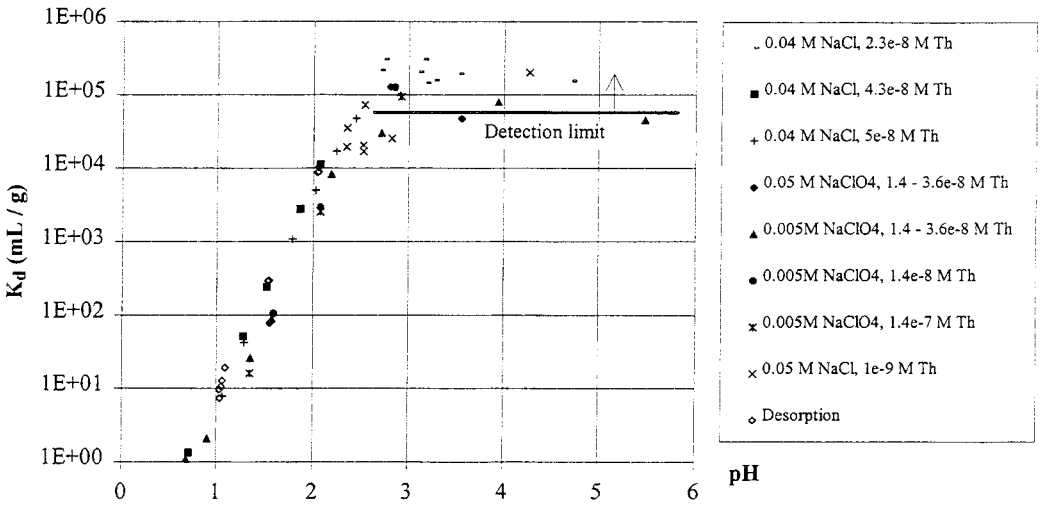

Figure 6.11 *The thorium sorption as a function of pH at various ionic strengths and Th concentrations. Above pH 3 the detection limit is reached and the experimental points refer to the least value of* K_d.

There were difficulties in modeling the thorium sorption. With the choice of surface site density (12 sites /nm^2) there was no difference in the slope for the different reactions modeled. However, decreasing the site density increased the difference in the slope between the different reactions. Below is a summary of the modeling of the thorium sorption with the different models available in FITEQL (CC, DLM, Stern and TLM) varying the site density and the number of protons released in the reaction. For each site density the surface acidity constants were recalculated (Table 6-7.)

Table 6-7. The resulting surface acidity constants for the varying site densities

Site density	pKa1	pKa2
1	4.4	8.0
5	3.9	8.6
10	3.6	8.8
12	3.5	8.9

In Table 6-8 the reactions modeled in FITEQL are presented. In all the models the Thorium forms an inner sphere complex with the titanium dioxide surface groups resulting in a charge at the 0-plane.

Table 6-8. The reactions used in FITEQL

	SOH	Ψ_0	Ψ_β	Ψ_d	Th4+	H+	Na+	Cl-
	1	**160**	**161**	**162**	**40**	**50**	**3**	**5**
CC	1	n	-	-	1	-m	0	0
DLM	1	n	-	-	1	-m	0	0
Stern	1	n	-n	-	1	-m	0	n
TLM	1	n	-n	0	1	-m	0	n

n + m = 4
m is the number of protons released in the reaction
n is the resulting charge on the surface

The next two pages present the resulting graphs for the different models. The number of protons released in the reaction modeled are in the leftmost column. In each figure the resulting relationships for the log K_d and pH are presented for three different site densities; 1,5 and 10 sites / nm^2. The page following the graphs contains the resulting constants. These will not be further commented. The observations from the graphs are summarized below.

Observations

For all the models there is a dependence for the resulting slope on the surface site density and the number of protons released. The smaller the surface site density the larger the difference in slope between the different modeled reactions. There is no large difference in the slopes for the higher surface site densities (5 and 10).

With the diffuse layer model the reaction can be fitted with the higher surface site densities as well. The reaction which fits the best is the one involving the release of 1 proton.

There is only a minor difference here between the double and triple layer model.

Conclusion

Since the site density has such a great impact on which reaction that fits the best this parameter has to be investigated further. At this stage the reaction that fits the best can not be determined since different site densities generates different slopes for the number

of protons released.

H^+	Constant Capacitance	Diffuse Layer Model
0	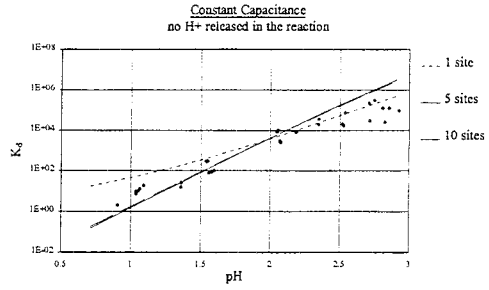	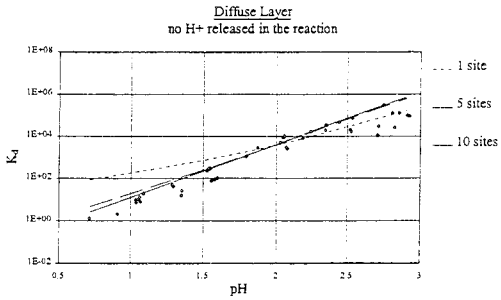
1	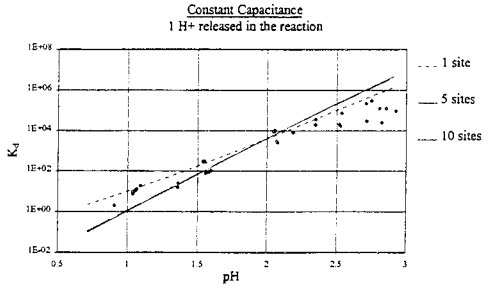	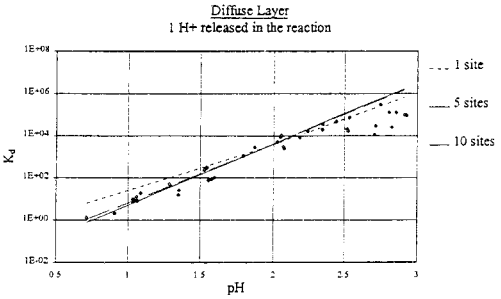
2	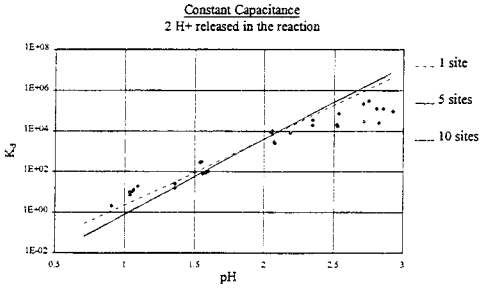	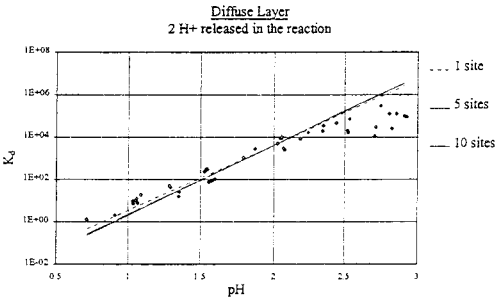
3	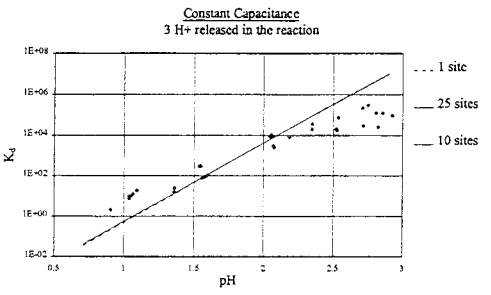	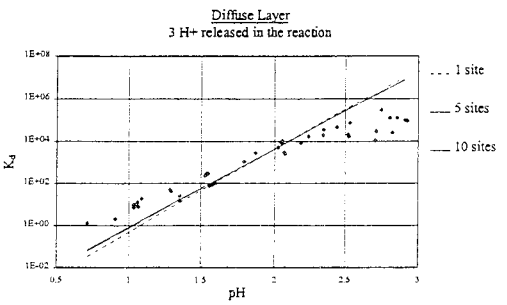
4	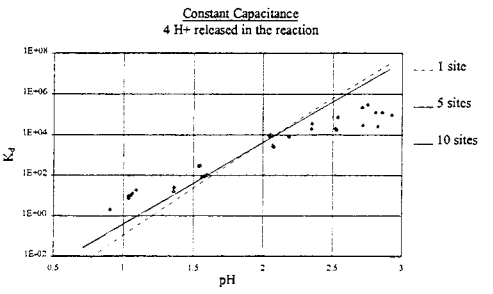	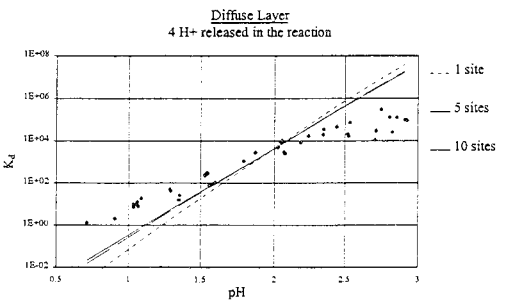

H^+	Stern	Triple Layer Model
0	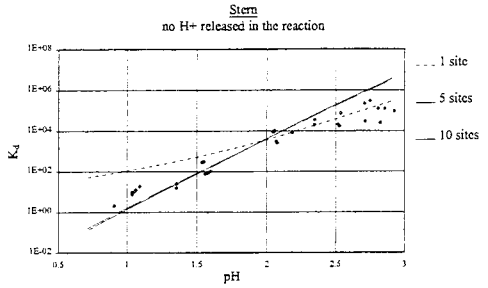	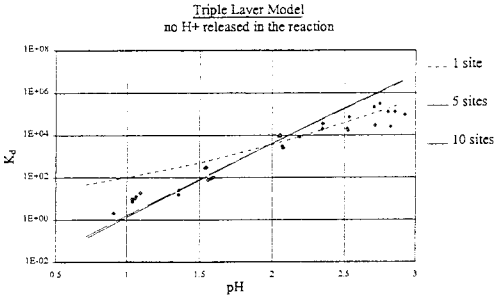
1	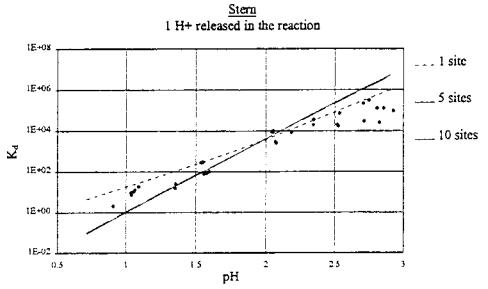	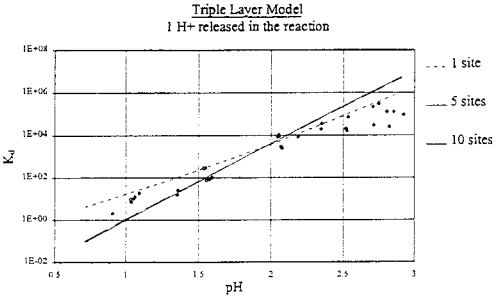
2	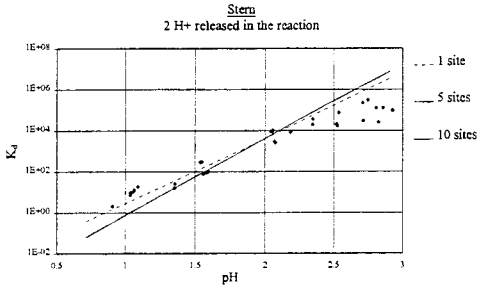	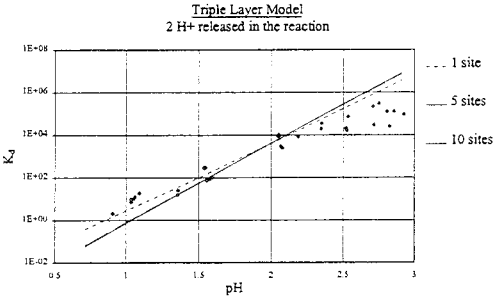
3	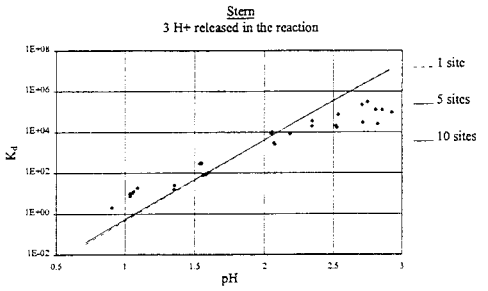	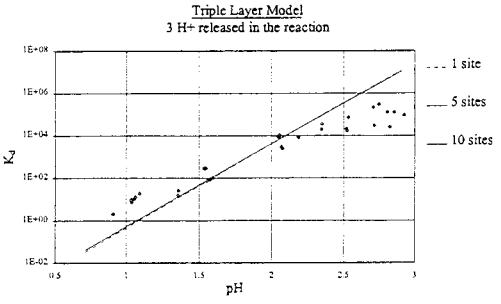
4	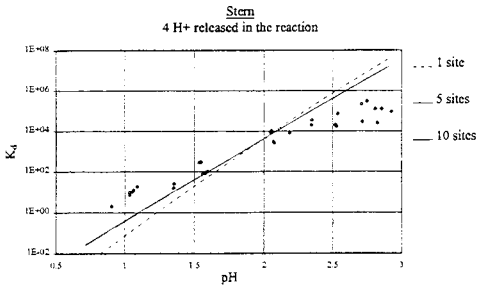	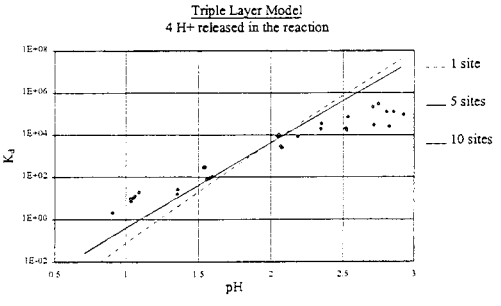

Table 6-9. The resulting surface complexation constants for Constant Capacitance Model

Site density	no H+ released	1 H+ released	2 H+ released	3 H+ released	4 H+ released
1	12.6	8.8	5.0	1.2	-2.6
5	13.8	9.4	5.0	0.5	-3.9
10	13.6	9.2	4.7	0.2	-4.2
12	13.6	9.1	4.6	0.2	-4.3

Table 6-10. The resulting surface complexation constants for Diffuse Layer Model

Site density	no H+ released	1 H+ released	2 H+ released	3 H+ released	4 H+ released
1	12.4	8.6	4.9	1.2	-2.5
5	13.1	8.8	4.6	0.4	-3.8
10	12.9	8.6	4.3	0.1	-4.2
12	12.8	8.6	4.3	-0.02	-4.3

Table 6-11. The resulting surface complexation constants for Stern Model

Site density	no H+ released	1 H+ released	2 H+ released	3 H+ released	4 H+ released
1	17.8	12.8	7.8	2.7	-2.3
5	19.7	13.8	7.9	2.0	-3.9
10	19.5	13.6	7.6	1.7	-4.2
12	19.4	13.5	7.6	1.6	-4.3

Table 6-12. The resulting surface complexation constants for Triple Layer Model

Site density	no H+ released	1 H+ released	2 H+ released	3 H+ released	4 H+ released
1	17.7	12.7	7.7	2.7	-2.3
5	19.6	13.7	7.9	2.0	-3.9
10	19.4	13.5	7.6	1.7	-4.2
12	19.3	13.4	7.5	1.6	-4.3

Sorption of U(VI) onto Al_2O_3

There is no significant difference observed in the sorption behavior for the different ionic strengths, electrolytes, experimental methods or uranium concentrations (see Figure 6.11). The independence of the sorption on the ionic strength indicates an inner sphere complexation with the alumina surface sites. The experimental independence on

uranium concentration indicate that there are no site heterogeneities.

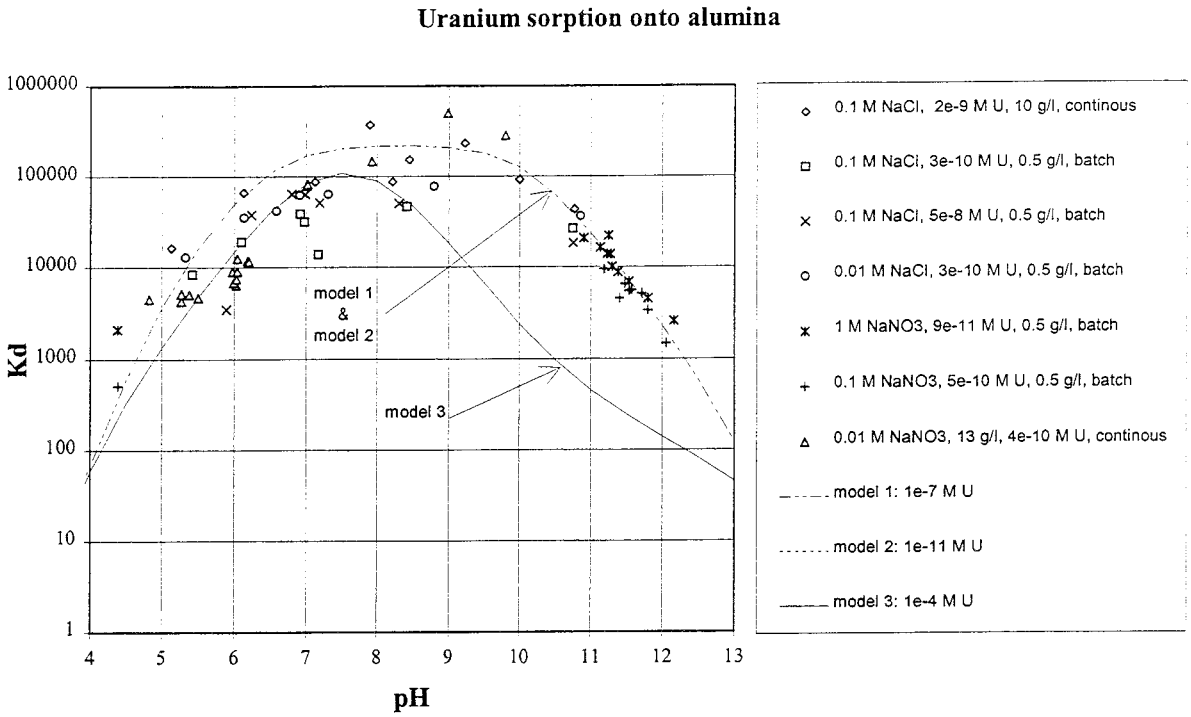

Figure 6.11 *K_d as a function of pH. The reactions and the constants used for the calculations are summarized in Table 6-12. (Note that models 1 and 2 overlap)*

The reactions used and the constants are summarized in Table 6-12. A good fit of the modeled uranium sorption was obtained using two reactions, a monodentate and a bidentate inner sphere. The stoichiometry for a bidentate inner sphere uranyl complex is identical to that of the monodentate attachment of a hydrolyzed uranyl ion (as suggested by /DeGueldre, Ulrich and Silby, 1994/ for americium). It is therefore impossible to differentiate between these structure on the basis of sorption measurements. The bidentate mechanism was chosen because there is spectroscopic evidence supporting the bidentate attachment of divalent cations onto alumina /Motschi, 1985/. Modeling using only the bidentate complexation gave equally good fit in the pH range studied but would not be able to predict the sorption at lower pH. EXAFS of U onto ferrihydrites indicate that a bidentate complex forms. Since the pK_{a2}s for the alumina and Fe oxides are so close (11.3 and 11.1 /Hayes, Papelis and Leckie, 1988/, respectively) the same surface complexation model should be applicable. The good fit, the EXAFS and the pK_{a2}s indicate that the bidentate binding is likely to be the dominating surface reaction.

Results of the modeling for three different uranium concentrations (10^{-7}, 10^{-11} and 10^{-4} M) are presented in Figure 6.11. The model did not predict any difference for the two lowest concentrations (Figure 6.11 model 1 and 2) but a rather large shift towards decreasing the K_d for the higher uranium concentration at the same pH (Figure 6.11 model 3). This effect was only due to the formation of polynuclear complexes in the solution. If there were polynuclear complexes formed with the surface the fraction sorbed would increase with increasing uranium concentrations. Therefore it seems unlikely that polynuclear complexes form with the surface.

Table 6-12. Reactions and constants for the uranium sorption onto alumina

Reaction	Constant		Reference
Acid dissociation of alumina surface:			
$SOH + H^+ \Leftrightarrow SOH_2^+$	$pK_{a1}^{int} = 7.2$		
$SOH \Leftrightarrow SO^- + H^+$	$pK_{a2}^{int} = 11.2$		
$SOH_2^+ + A^- \Leftrightarrow SOH_2^+ A^-$	$K_{A^-}^{int} = 0$		
$SO^- + Na^+ \Leftrightarrow SO^- Na^+$	$K_{Na^+}^{int}=15$		/Rundberg, Albinsson and Vannerberg, 1994/
Aqueous uranium speciation	original	adjusted	
$UO_2^{2+} + H_2O \Leftrightarrow UO_2(OH)^+ + H^+$	-4.9	-4.9	/Grenthe *et.al.* 1992/
$UO_2^{2+} + 2\ H_2O \Leftrightarrow UO_2(OH)_2 + 2H^+$	-9.7	-11.4	/Grenthe *et.al.* 1992/
$UO_2^{2+} + 3\ H_2O \Leftrightarrow UO_2(OH)_3^- + 3H^+$	-18.3	-21.5	/Grenthe *et.al.* 1992/
$UO_2^{2+} + 4\ H_2O \Leftrightarrow UO_2(OH)_4^{2-} + 4H^+$	-31.8	-34.5	/Grenthe *et.al.* 1992/
$2\ UO_2^{2+} + H_2O \Leftrightarrow (UO_2)_2(OH)^{3+} + H^+$	-2.4	-2.4	/Grenthe *et.al.* 1992/
$2\ UO_2^{2+} + 2\ H_2O \Leftrightarrow (UO_2)_2(OH)_2^{2+} + 2H^+$	-5.02	-5.02	/Grenthe *et.al.* 1992/
$3\ UO_2^{2+} + 4\ H_2O \Leftrightarrow (UO_2)_3(OH)_4^{2+} + 4H^+$	-10.7	-10.7	/Grenthe *et.al.* 1992/
$3\ UO_2^{2+} + 5\ H_2O \Leftrightarrow (UO_2)_3(OH)_5^+ + 5H^+$	-14.05	-14.05	/Grenthe *et.al.* 1992/
$3\ UO_2^{2+} + 7\ H_2O \Leftrightarrow (UO_2)_3(OH)_7^- + 7H^+$	-28.9	-28.9	/Grenthe *et.al.* 1992/
$4\ UO_2^{2+} + 7\ H_2O \Leftrightarrow (UO_2)_4(OH)_7^+ + 7H^+$	-19.8	-19.8	/Grenthe *et.al.* 1992/
Surface complexation			
$SOH + UO_2^{2+} \Leftrightarrow SOUO_2^+ + H^+$	-3.1		
$2\ SOH + UO_2^{2+} \Leftrightarrow (SO)_2UO_2 + 2H^+$	3.4		

Inner layer capacitance:	1.1 C/m^2	Site density:	10 sites / nm^2
Outer layer capacitance	0.2 C/m^2	pKw:	13.7
Surface area (BET):	142.9 m^2/g	I:	0.1 M

7 Conclusions

Titrations

The calibration is of uttermost importance in the calculations of the constants since the difference in the concentration is the ingoing parameter in both the determination of the surface charge and the apparent equilibrium constant. Since the washed titanium dioxide appears to be clean (good agreement between the pH_∞ and pH_{pzc}) and the curves intersect close to $\sigma = 0$, the calibration appears to be good.

Pure titanium dioxide gives a pK^{app} that has a very linear dependence on the inner surface charge. This shows that it is a fair estimation to assume a linear relationship between the inner surface charge and the potential as is done in models such as CCM, DLM and TLM. From the slope the capacitance of the inner layer can be calculated. The magnitude of the values of the capacitances from the titrations agree well with other proposed in the literature /Hayes, Redden, Ela and Leckie, 1991/.

Data close to pH_{pzc} can not be used to calculate the apparent equilibrium constants as the assumption that either the positive or negative sites dominate gives rise to pK^{app} that approach infinity. The extrapolation method outlined here is in most parts similar to the double extrapolation method proposed by Davis, James and Leckie [DAV 78]. Therefore the same limits in calculating the apparent equilibrium constants should apply using their method.

Sorption

The relationship between the K_d and the equilibrium constant of the reaction can be used to infer the number of protons released in the surface complexation reaction and thus to infer the stoichiometry of the reaction. This relationship might also be useful in making predictions of the sorption behavior at varying pH with the knowledge of the K_d and the reaction.

There is no difference in the results from the different methods employed here. The on-line sorption has the advantage that the pH can be determined more accurately by using two electrodes instead of a combination electrode, and the desorption can easily be studied by varying the conditions without affecting the experiments.

TiO_2
Np, Th and Co form inner sphere complexes with the titanium dioxide surface.
The neptunyl ion forms a neutral complex, indicated by the +1 slope between the log K_d and the pH.

Cobalt forms a complex either with the first hydrolyzed species or directly with the oxygen of the TiO_2. Since this complex is charged it will be affected by the charge of the surface; below the point of zero charge the sorption will be diminished and above it

will be enhanced. This results in a slope of 1.5 in a plot of log K_d versus pH.

The thorium can be modeled with a combination of different site densities and number of protons released. To be able to determine which reaction is the most probable the surface site density has to be further investigated and better determined.

Alumina
We could model the sorption of uranium as an inner sphere bidentate complex with the alumina surface, with a maximum sorption at pH 8-9. There are no low density high energy sites affecting the surface complexation of uranium at low concentrations ($9x10^{-11}$ - $5x10^{-8}$ M).

The same surface complexation model should be applicable to iron oxides because the pK_{a2}s are so close. The observed sorption is found to be in close agreement with that observed for uranium onto goethite /Hsi and Langmuir, 1985/ when the surface area differences are taken into account. The observation of /Bradbury and Baeyens, 1993/ that the surface complexation of neptunyl on many aluminosilcate minerals and rocks can be modeled as iron oxide surfaces may be a consequence of this property of alumina.

The dependence of the surface complexation constant on the pK_{a2} of the metal oxide needs to be further explored to develop a quantitative model. The bidentate surface complex will have a different dependence on pK_{a2} from the monodentate complex. Uranyl surface complexation needs to be studied on more acidic metal oxides, such as silicon dioxide. Further spectroscopic studies of the structure of the uranyl surface complex are needed to complement the sorption experiments.

Future work

A continuation of this work is planned and will include:
- Measurements of isotherms to investigate the influence of the concentration on the sorption.
- Sorption studies of a trivalent cation (e.g. Pm) and an anion (PO_4^{3-}) onto TiO_2 to further investigate the influence of the oxidation state.
- Sorption studies at varying carbonate concentrations.
- Further studies of the relationship between the K_d, the pH and the equilibrium constant of the surface complexation reaction.
- Comparison of the sorption behavior to minerals of other pH_{pzc}.
- Sensitivity analysis and comparison between different codes.
- Determination of the surface site density.

8 Applicability

Surface complexation studies as described here have at least three different purposes: i) to provide data for validation of the surface complexation models ii) to provide qualitative information of how different factors such as pH, ionic strength, temperature and complexing ligands (for example carbonates and phosphates) will affect the sorption iii) to provide surface complexation constants and reactions to be used in quantitative predictions of the sorption in complex geochemical systems modelling.

Validation of the models

There are a number of different models of varying complexity (from simple models without electrostatics to quadruple layer models). However, if a model is to be used in a complex system predicting the sorption behavior of various radionuclides it has to be validated using simple systems first. Therefore it is essential with good experimental data from systems that are relatively simple.

In this work we have used the triple layer model. With this model we were able to model the sorption behavior of Np and Co but, even though the system was simple and very well defined, we have not yet been able to model the results from the thorium sorption satisfactorily using the simple approach (one reaction with the surface, one type of surface sites).

There are a number of different ways of modeling data: one may include a number of different possible reactions. We have tried to keep it as simple as possible and not include reactions which we do not find plausible. Several authors in the literature add two different types of sites; weak and strong sites. However, in this work one type of site was enough to describe the sorption.

Information provided directly from the surface complexation studies

A number of important qualitative informations can be gained directly from the surface complexation studies such as the effect on the sorption of:
- pH
- ionic strength
- temperature
- concentration of complexing ligands such as carbonate and phosphate.

In addition the reversibility of the reaction can be studied.

Incorporation of surface complexation in geochemical models

A few codes such as CHEQMATE /Haworth, Sharland, Tasker and Tweed, 1988/, have coupled sorption described as surface complexation and transport models. /Sposito,

1982/ pointed out that a number of different models can represent the same set of adsorption data equally well but the corresponding chemical parameters in the models can have quite different values. One example of this is the fairly large difference in the constant for the formation of a complex between the neptunyl and goethite for the same set of data from /Girvin, Ames, Schwab and McGarrah, 1991/ reinterpreted by /Bradbury and Bayens, 1993/ changing the pK from 3.2 to -0.98 by using the generalized two-site model and thus introducing two different energy sites (strong and weak sites). This indicates that the surface complexation constants should be used with some care. An intercomparison between the strength of different complexes is at this point hard to make since there are so many different models flourishing. In addition, the values of the constants are highly dependent on the choice of reactions, the surface site density, the concentration of weak and strong surface sites, the surface complexation model and on the model parameters (the capacitance etc.)

There are however several examples where surface complexation has been used to predict the sorption in natural systems. /Bradbury and Bayens, 1993/ for example predicted the sorption of Np onto igneous rock from the surface complexation of Np with goethite. /Koss, Winkler and Bütow, 1992/ predicted the sorption of some cations based on surface complexation data from the EIR data base and data from Gorleben. They used a surface complexation model that did not include electrostatics for predicting the sorption of several cations in sediments with a known composition and cation exchange capacity. /Davis, 1997/ have applied laboratory derived surface complexation model for zinc adsorption to field observations of the transport of Zn in ground water. They concluded from this study that surface complexation may be a valuable tool for predicting the sorption under variable chemical conditions. The CHEQMATE has been used by /Brown, Haworth, Sharland and Tweed, 1991/ to model the progress of some radionuclides through a porous material using surface complexation data from batch sorption experiments.

These types of intercomparisons should always be done with some precaution though. The original data which Bradbury Bayens modeled were not intended for these types of models and a number of parameters were not measured. Despite this they reached a fair agreement and one might argue that in a natural system the same type of simplifications that were made have to be made.

9 Acknowledgments

Studsvik is gratefully acknowledged for ICP-MS measurements of the Th concentration. Prof. Jan-Olov Liljenzin is gratefully acknowledged for his valuable help.

10 References

Y. Albinsson, C. Ekberg, 1998, A method for preparing of ^{234}Th, In Prep.

B. Allard, H. Kipatsi, J. Liljenzin 1980, Expected Species of Uranium, Neptunium, and Plutonium in Neutral Aqueous Solutions, J. Inorg. Nucl. Chem., 42, 1015-1027

C.F. Baes and R.E. Mesmer 1986, The hydrolysis of Cations, John Wiley and Sons Inc., New York,

R. Bates 1973, Determination of pH THEORY AND PRACTICE, John Wiley and Sons, New York,

Y.G. Bérubé and P. L.de Bruyn 1968, Adsorption at the Rutile-Solution Interface II. Model oif the Electrochemical Double Layer, J. Coll. Interface. Sci., 27 ,305,

M.H Bradbury and B. Bayens 1993, A General Application of Surface Complexation to Modeling Radionuclide Sorption in Natural Systems, J. Coll. Interface Sci., 128, 364-371,

P.L. Brown, A. Haworth, S.M. Sharland, C.J. Tweed 1991, Modeling Studies of the Sorption of Radionuclides in the Far Field of a Nuclear Waste Repository, Radiochim. Acta 52/53, 439-443

T. Carlsson 1994, Surface Complexation in TiO_2 suspensions, A laboratory study, VTT Research Notes, 1617

J. A. Davis, R. O. James, J. O. Leckie 1978, Surface Ionization and Complexation at the Oxide/Water Interface, I. Computation of Electrical Double Layer Properties in Simple Electrolytes, J. Coll. Interface Sci., 63, 3

J .A. Davis 1997 NEA International Meeting on Chemical Modelling of Sorption in the Field of Radioactive Waste Management, May6-8, Oxford, UK

C. DeGueldre, H. J. Ulrich and H. Silby 1994, Sorption of ^{241}Am onto Montmorillonite, Illite and Hematite Colloids, Radiochim. Acta 65, 173-179

D.A. Dzombak and F. M. M. Morel 1990, Surface Complexation Modeling: Hydrous Ferric Oxide, John Wiley and Sons, New York

D. Girvin, L. Ames, A. Schwab, J. McGarrah 1991, Neptunium Adsorption on Synthetic Amorphous Iron Oxyhydroxide, J. Coll. Interface Sci., 141, 67-78

D.C. Grahame 1947, The Electrical Double Layer and the Theory of Electrocapillary, Chem. Rev., 41, 441-501

G.Gran 1950, Determination of the Equivalent Point in Potentiometric Titrations, Acta Chemica Scandinavia 4, 559-557

G.Gran 1952, Determination of the Equivalence Point in Potentiometric Titrations. Part II, International Congress on Analytical Chemistry, 77, 661-671

I. Grenthe, J. Fuger, R. J. M. Konings, R. J. Lemire, S. B. Muller, C. Nguyen-Trung and H. Wanner, 1992, Chemical Thermodynamics of Uranium **1992**, (H.. Wanner and I. Forest, eds) Elsevier Sci. Publ., Amsterdam

K.F. Hayes and J.O. Leckie 1987, Modeling Ionic Strength Effects on Cation Adsorption at Hydrous Oxide/Solution Interfaces, J. Coll. Interface Sci. 115, 2

K.F. Hayes, C. Papelis and J.O. Leckie 1988, Modeling Ionic-Strength Effects on Anion Adsorption at Hydrous Oxide Solution Interfaces, J. Coll. Interface Sci. 125(2), 717-726

K.F. Hayes, G. Redden, W. Ela, J.O. Leckie 1991, Surface Complexation models: An Evaluation of Model Parameter Estimation Using FITEQL and Oxide Mineral Titration Data, J. Coll. Interface Sci., 142, 2

A. Haworth, S.M. Sharland, P.W. Tasker and C.J. Tweed 1988 , A Guide to the Coupled Chemical Equilibria and Migration Code CHEQMATE, Harwell Laboratory Report NSS-R113

C-K.D. Hsi and D. Langmuir 1985, Geochim. Cosmochim. Acta 49, 1931-1941

C- Huang, W. Stumm 1973, Specific Adsorption of Cations on Hydrous γ-Al_2O_3 J. Coll. Interface Sci., 43, 409-420

R.O. James, P.J. Stiglich, T.W. Healy 1981, The TiO_2/Aqueous Electrolyte System - Applications of Colloid Models and Model Colloids, Adsorption from Aqueous Solutions, P.H. Tewari, Plenum Press, New York

M.J.G. Janssen and H. N. Stein 1986, The TiO2/Electrolyte Solution Interface I. Influence of Pretreatment Conditions and of Impurities, J. Coll. Interface Sci., 109, 2

V. Koss, A. Winkler, E. Bütow 1992, Experimental Investigation and Modelling of the Migratrion of Radionuclides from the Ellweiler Uranium Mill Tails, Radiochim. Acta, 58/59, 447-451

Ch. Lierse, W. Trieber and J.I. Kim, 1985, Hydrolysis Reactions of Neptunium(V), Radiochim. Acta 38, 27-28

M.L. Machesky and M. A. Anderson 1986, Calorimetric Acid-Base Titration of Aqueous Goethite and Rutile Suspensions, Langmuir, 2, 582-587

N. Marmier, J. Dumonceau, J. Chupeau, F. Fromage 1994, Influence des contraintes

électrostatiques sur la sorption de l'ytterbium trivalent sur l'alumine, C. R. Acad. Sci. Paris, 318, II, 177-183

H. Motschi, 1985, Adsorption Sci. and Technology, 2, 39-54

J. Noh and J. Schwarz 1989, Estimation of the Point of Zero Charge of Simple Oxides by Mass Titration, J. Coll. Interface Sci., 130, 1

K.S. Pitzer 1991, Activity Coefficients in Electrolyte Solutions, 2nd ed, CRC Press, Boca Raton, USA, [ROS 65] **F.J.C. Rossotti, H. Rossotti 1965**, Potentiometric Titrations Using Gran Plots A Textbook omission, J. of Chemical Education, 42, 7

R. S. Rundberg 1996, unpublished work.

R.S. Rundberg, Y. Albinsson, K. Vannerberg 1994, Sodium Adsorption onto Goethite as a Function of pH and Ionic Strength, Radiochim. Acta 66/67, 333-339

J.R. Rustad, A.R. Felmy, B P. Hay 1996, Molecular Statiscs Calculations of Proton Binding to Goethite Surfaces: A New Approach to Estimation of Stability Constants for Multisite Surface Complexation Models, Geochim. et Cosmochim. Acta, vol 60, no 9, pp. 1563-1576

S. Sherif, 1997, Development of a Method for Determination of Aluminium in Water, Diploma work, Dept. of Nuclear Chemistry, Chalmers University of Technology

G. Sposito 1983, On the Surface Complexation Model of the Oxide-Aqueous Solution Interface, J. Coll. Interface Sci. 91, 2

R. Sprycha 1986, Zeta Potential and Surface Charge Components at Anatase/Electrolyte Interface, J. Coll. Interface Sci., 110 (1)

R. Sprycha 1989, Electrical Double Layer at Alumina/Electrolyte Interface II Surface Charge and Zeta Potetial, J. Coll. Interface Sci., 127, 1-11

R. Sprycha 1989, Electrical Double Layer at Alumina/Electrolyte Interface II Adsorption of Supporting Electrolyte Ions, J. Coll. Interface Sci., 127, 12-25

D.A. Sverjensky 1994, Zero-point-of-charge Prediction from Crystal Chemistry and Solvation Theory, Geochim. et Cosmochim. Acta, 58, 4, 3123-3129

C. V. Toner, D. L. Sparks 1995, Chemical Relaxation and Double Layer Model Analysis of Boron Adsorption on Alumina, Soil. Sci. Soc. Am. J. 59:395-404

D.E. Yates 1975 , Ph.D. Thesis , University of Melbourne, Australia,

S. Zalac and N. Kallay 1992, Application of Mass Titration to the Point of Zero Charge Determination, J. Coll. Interface Sci., 149, 1

Z.Z. Zhang, D. L. Sparks, N. C. Scrivner 1994, Characterization and Modeling of the Al-oxide/Aqueous Solution Interface, J. Coll. Interface Sci.,162, 244-251,

J. Westall 1982, FITEQL, A Computer Program for Determination of Chemical Equilibrium Constants from Experimental Data, Report 82-01 Dept. of Chemistry, Oregon State University, Corvallis Oregon

G. R. Wiese, T.W. Healy 1975, Adsorption of Al(III) at the TiO_2-H_2O Interface, J. Coll. Interface Sci., 51, 3,

Appendix I

List of symbols

pH_{pzc}		point of zero charge
pH_{∞}		the pH which a solution approaches as the mass concentration increases
pH_{iep}		the isoelectric point; i.e. the pH at which the electrophoretic mobility is zero
$\equiv SOH$		surface sites
$\{i\}$		activity of a species *i*
K^{int}		the intrisic equilibrium constant
K^{app}		the apparent equilibrium constant (referring to the bulk concentrations)
K_d		distribution coefficient
K_{A^-}, K_{X^+}		constants for outer sphere complexation of an anion (A^-) and cation (X^+) with the surface
k'		surface site density
Ψ_i		potential difference between the bulk and a plane *i* where *i* is 0, β, d
σ		charge
C		capacitance
z		charge of a species
$[l_i]$		concentration of a species *l* which with the suffix *i* denotes:
	add	the conc. from the amount added
	bulk	the conc. in the bulk of the aqueous phase
	tot	the total conc.
$[l]_i$		concentration of a species *l* which with the suffix *i* denotes:
	aq	the conc. of the unhydrolyzed species
	totaq	the total conc. in the bulk of the aqueous phase
$\Delta[H^+]$		difference between added amount of H+ and measured due to amphoteric reaction of surface
Q_w		water ionization product (function of the ionic strength)
K_w		water dissociation constant
c_a		concentration of the acid
c_b, c'_b		concentration of the base determined from the acid and base side
v_a, v_b		volume added acid and base
v_e, v'_e		equivalence volume at acid and base side
v_{tot}		total volume

E	electrode potential
$E_{R.E.}$	reference electrode potential
$E_{G.E.}$	glass electrode potential
E_j	liquid junction potential
$E^o_{G.E}, E^o_j$	standard potentials
E^o	constant ($= E^o_j + E^o_{G.E} + E_{R.E.}$)
E_0	constant for the acid side at a certain ionic strength
E'_0	constant for the base side at a certain ionic strength
$\overline{E_0}, \overline{E'_0}$	the average potentials from the calibration on the acid and base side
$E_{meas,n}$	measured potential
$E_{calc,n}$	the calculated value of the potential
Φ	liquid junction potential coefficient
F_1, F_2	Gran functions
γ_i	activity factor of a species *i*
η	the efficiency of the electrode
F	Faraday constant
R	Molar gas constant
T	absolute temperature
s	=RT/F ln10
S_{mol}	site density in mol sites per mass
S_m	surface area per unit mass
S_V	surface area of solid in suspension per volume
m	mass
N_A	Avogadros number
N_S	site denisty (sites / nm^2)
V	volume

List of SKB reports

Annual Reports

1977-78
TR 121
KBS Technical Reports 1 – 120
Summaries
Stockholm, May 1979

1979
TR 79-28
The KBS Annual Report 1979
KBS Technical Reports 79-01 – 79-27
Summaries
Stockholm, March 1980

1980
TR 80-26
The KBS Annual Report 1980
KBS Technical Reports 80-01 – 80-25
Summaries
Stockholm, March 1981

1981
TR 81-17
The KBS Annual Report 1981
KBS Technical Reports 81-01 – 81-16
Summaries
Stockholm, April 1982

1982
TR 82-28
The KBS Annual Report 1982
KBS Technical Reports 82-01 – 82-27
Summaries
Stockholm, July 1983

1983
TR 83-77
The KBS Annual Report 1983
KBS Technical Reports 83-01 – 83-76
Summaries
Stockholm, June 1984

1984
TR 85-01
Annual Research and Development Report 1984
Including Summaries of Technical Reports Issued during 1984. (Technical Reports 84-01 – 84-19)
Stockholm, June 1985

1985
TR 85-20
Annual Research and Development Report 1985
Including Summaries of Technical Reports Issued during 1985. (Technical Reports 85-01 – 85-19)
Stockholm, May 1986

1986
TR 86-31
SKB Annual Report 1986
Including Summaries of Technical Reports Issued during 1986
Stockholm, May 1987

1987
TR 87-33
SKB Annual Report 1987
Including Summaries of Technical Reports Issued during 1987
Stockholm, May 1988

1988
TR 88-32
SKB Annual Report 1988
Including Summaries of Technical Reports Issued during 1988
Stockholm, May 1989

1989
TR 89-40
SKB Annual Report 1989
Including Summaries of Technical Reports Issued during 1989
Stockholm, May 1990

1990
TR 90-46
SKB Annual Report 1990
Including Summaries of Technical Reports Issued during 1990
Stockholm, May 1991

1991
TR 91-64
SKB Annual Report 1991
Including Summaries of Technical Reports Issued during 1991
Stockholm, April 1992

1992
TR 92-46
SKB Annual Report 1992
Including Summaries of Technical Reports Issued during 1992
Stockholm, May 1993

1993
TR 93-34
SKB Annual Report 1993
Including Summaries of Technical Reports Issued during 1993
Stockholm, May 1994

1994
TR 94-33
SKB Annual Report 1994
Including Summaries of Technical Reports Issued during 1994
Stockholm, May 1995

1995
TR 95-37
SKB Annual Report 1995
Including Summaries of Technical Reports Issued during 1995
Stockholm, May 1996

1996
TR 96-25
SKB Annual Report 1996
Including Summaries of Technical Reports Issued during 1996
Stockholm, May 1997

List of SKB Technical Reports 1998

TR 98-01
Global thermo-mechanical effects from a KBS-3 type repository. Summary report
Eva Hakami, Stig-Olof Olofsson, Hossein Hakami, Jan Israelsson
Itasca Geomekanik AB, Stockholm, Sweden
April 1998

TR 98-02
Parameters of importance to determine during geoscientific site investigation
Johan Andersson[1], Karl-Erik Almén[2], Lars O Ericsson[3], Anders Fredriksson[4], Fred Karlsson[3], Roy Stanfors[5], Anders Ström[3]
[1] QuantiSci AB
[2] KEA GEO-Konsult AB
[3] SKB
[4] ADG Grundteknik KB
[5] Roy Stanfors Consulting AB
June 1998

TR 98-03
Summary of hydrochemical conditions at Aberg, Beberg and Ceberg
Marcus Laaksoharju, Iona Gurban, Christina Skårman
Intera KB
May 1998

TR 98-04
Maqarin Natural Analogue Study: Phase III
J A T Smellie (ed.)
Conterra AB
September 1998

TR 98-05
The Very Deep Hole Concept – Geoscientific appraisal of conditions at great depth
C Juhlin[1], T Wallroth[2], J Smellie[3], T Eliasson[4], C Ljunggren[5], B Leijon[3], J Beswick[6]
[1] Christopher Juhlin Consulting
[2] Bergab Consulting Geologists
[3] Conterra AB
[4] Geological Survey of Sweden
[5] Vattenfall Hydropower AB
[6] EDECO Petroleum Services Ltd.
June 1998

TR 98-06
Indications of uranium transport around the reactor zone at Bagombe (Oklo)
I Gurban[1], M Laaksoharju[1], E Ledoux[2], B Made[2], A L Salignac[2],
[1] Intera KB, Stockholm, Sweden
[2] Ecole des Mines, Paris, France
August 1998

TR 98-07
PLAN 98 – Costs for management of the radioactive waste from nuclear power production
Swedish Nuclear Fuel and Waste Management Co
June 1998

TR 98-08
Design premises for canister for spent nuclear fuel
Lars Werme
Svensk Kärnbränslehantering AB
September 1998

TR 98-09
Test manufacturing of copper canisters with cast inserts Assessment report
Claes-Göran Andersson
Svensk Kärnbränslehantering AB
Augusti 1998

TR 98-10
Characterization and Evaluation of Sites for Deep Geological Disposal of Radioactive Waste in Fractured Rocks
Proceedings from The 3rd Äspö International Seminar, Oskarshamn, June 10–12, 1998-11-10
Svensk Kärnbränslehantering AB
September 1998

TR 98-11
Leaching of 90-year old concrete mortar in contact with stagnant water
Jan Trägårdh, Björn Lagerblad
Swedish Cement and Concrete Research Institute
July 1998

TR 98-12
Geological structural models used in SR 97
Uncertainty analysis
Pauli Saksa, Jorma Nummela
FINTACT Ltd
October 1998

TR 98-13
Late Quaternary changes in climate
Karin Holmgren and Wibjörn Karlén
Department of Physical Geography
Stockholm University
December 1998

TR 98-14
Partitioning and transmutation (P&T) 1997
Åsa Enarsson, Anders Landgren, Jan-Olov Liljenzin, Mats Skålberg, Lena Spjuth
Department of Nuclear Chemistry, Chalmers University of Technology, Gothenburg
and
Waclaw Gudowski, Jan Wallenius
Department of Nuclear and Reactor Physics, Royal Institute of Technology, Stockholm
May 1998